# Expression of Recombinant Zika Virus-Like Particles

# in *Nicotiana benthamiana*

by

Michelle Di Palma

A Thesis Presented in Partial Fulfillment
of the Requirements for the Degree Master of Science

Approved July 2018
Graduate Supervisory Committee:
Tsafrir Mor, Chair
Hugh Mason
Joseph Blattman

ARIZONA STATE UNIVERSITY

August 2018

ABSTRACT

Zika virus (ZIKV) outbreaks have been linked to several neurological pathologies in the developing fetus, which can progress to spontaneous abortion and microcephaly in newborns whose mothers were infected with the virus during pregnancy. ZIKV has also been correlated with neurological complications in adults such as Guillain-Barré Syndrome (GBS). ZIKV outbreaks often occur in low income areas with limited access to healthcare. Therefore, there is a need to create a low-cost preventative vaccine against the virus. Mature ZIKV particles contain a lipid bilayer, a positive sense single stranded RNA genome and three structural proteins: the envelope (E), membrane (M) and capsid (C) proteins. Congruently, to other members of the Flaviviridae family, ZIKV proteins are synthesized as a polyprotein precursor which needs to be processed to release the mature structural and non-structural viral proteins. Past studies have determined the ZIKV precursor protein is cleaved by a host furin protease which separates the Pr peptide and the M protein, while the host signal peptidase separates the M and E protein. Processing is important for correct folding of the E protein. In turn, the most important neutralizing antibodies upon infection are directed against epitopes of the E protein. In this work, we used a Bean Yellow Dwarf Viral vector system to transiently express, in *Nicotiana benthamiana* plants, a portion of the ZIKV polyprotein encoding the Pr, M and E proteins. I further demonstrate that plants can proteolytically process the polyprotein to yield the two integral membrane proteins M and E. These proteins can be shown to co-partition into a soluble membrane-particulate fraction, consistent with formation of enveloped virus-like particles (VLPs). This work provides the first step in creating a low-cost sustainable plant-based production system of ZIKV VLPs that can be explored as a potential component of a low-cost prophylactic vaccine against ZIKV.

DEDICATION

I am dedicating this to my parents, my brother and my two sisters. You all mean the world to me and I will always try my hardest in everything I do for you all. You inspire me to strive to be a better person in so many ways and to always love those around me unconditionally. Thank you for believing in me, I love you with all my heart.

ACKNOWLEDGMENTS

I would like to thank Tsafrir Mor for letting me work in his lab for the last few years. Thank you for encouraging me and for taking the time to exchange ideas with me that help me see the world from a different perspective. Thank you for being honest about my work and helping me realize small failures might not be as big of a deal as they might seem at the time. You have a sincere interest in the success of your students, it is refreshing, and it inspires me to try harder. Thank you to Hugh Mason for designing the initial vector used in this study and for answering any question I had with a sincere want to help me better understand the project.

I can't thank Andy Diamos enough. Thank you for helping me through cloning and teaching me technique that helped me solve my lab mistakes and hopefully will do the same for the future. Thank you for always being positive and for being encouraging in everything I do. Thank you to Mary Pardhe for allowing me to utilize your Zika monoclonal antibody. Your antibody allowed me to gather all initial data and without it I would likely not have continued my project. You are so kind and I am honored to be able to work and learn with you. Thank you to Joseph Hunter for teaching me gradient techniques and for giving me encouragement and pointers all along the way. Thank You to Lydia Meador for teaching me the initial techniques needed to conduct research. Thank You to Siavosh who initially began researching this project with me. Thank You to everyone previously not mentioned in Mor lab, especially Rebecca, Aigerim, Boston and Sierra. You all inspire me to work harder and smarter. Thank you to everyone in Mason lab previously not mentioned, Sara, Brandon, Art and Matt. I love everyone in both labs and am always inspired by you.

Thank you to everyone on my committee for being a part of it, even if I already mentioned you. Thank You to Tsafrir Mor, Hugh Mason, and Joseph Blattaman. I enjoyed your classes and without the knowledge provided by them and exposure to ideas regarding the application of that knowledge, I would likely never have wanted to go into research and would be considering different future plans.

Thank you to Wendi Simonson for being the most amazing graduate student advocate! Finally, thank you to the Graduate Student Professional Association (GPSA) for believing in my project and giving me grant money to help me achieve its success.

TABLE OF CONTENTS

LIST OF FIGURES

FIGURE Page

LIST OF TABLES

# 1. INTRODUCTION

Recent outbreaks of Zika Virus (ZIKV) in the Americas revealed the virus as a strong cause of malformation in infected human embryos. It is shown to be the source of various neurodevelopmental birth defects, including microcephaly as well as spontaneous abortions (Hasan *et al.*, 2018). Many of these outbreaks have occurred in areas with limited access to medical care and low-capital, capital which would allow affected countries to bring treatments, for the virus and virus-associated febrile symptoms, in from other areas (United Nations Development Programme, 2017). Though outbreaks of the virus have progressively become less common, RNA viruses, like ZIKV, can change their virulence patterns and means of transmission more often than DNA viruses. Therefore, ZIKV remains a public-health concern as it could reemerge in the future (Monath, 2018).

Since there is no current FDA approved vaccine against the virus, researchers have been working to develop a vaccine against ZIKV should the necessity appear (Abbink *et al.*, 2018). While the efficacy and safety of such a vaccine are clearly the major objectives, it is imperative such a vaccine candidate be inexpensively and sustainably manufactured. This study aims to investigate a possible method to achieve this goal.

## *1.1 History of Zika Virus*

ZIKV is a member of the *Flaviviridae* family and was first isolated in 1947 in the Zika Forest of Uganda (Dick, 1952; Dick *et al.*, 1952). The virus did not produce many observable side effects for those who contracted it, so it often went ignored and undiagnosed (Bearcroft, 1956; Simpson, 1964). In January of 1948, the same group of researchers who initially isolated the virus trapped mosquitoes from the same place where the virus was originally located. Again, they isolated the virus, but this time from the infected mosquitoes, and characterized the previously unrecorded virus as “Zika

Virus" (Dick *et al.*, 1952). Years later, manifestations of previously recorded ZIKV symptoms appeared in patients who also began to develop jaundice, leading people to believe that ZIKV caused jaundice as well. In 1954, William Beacroft found evidence supporting that ZIKV was not a contributing factor to jaundice by injecting himself with the virus and recording his symptoms. He had no symptoms of jaundice and compared his findings to another patient who also did not develop jaundice upon infection with ZIKV (Bearcroft, 1956). Intermittent reports of the virus were present in lab workers as well as a few laymen through the following years. Many countries, such as Malaysia and Indonesia, in the 1970's and 1980's began to report scattered virus in mosquitoes, animals and rarely in humans (Garcia *et al.*, 1969; Olson *et al.*, 1981). In 2007 physicians reported an outbreak of an illness on Yap Island in the Federated Republic of Micronesia, characterized by rash, conjunctivitis (inflammation of the conjunctiva resulting in "pinkeye") and arthralgia (joint pain). Serum from these patients contained IgM antibodies that cross-reacted against Dengue virus (DENV), although the illness seemed clinically distinct from DENV (Duffy *et al.*, 2009; Petersen *et al.*, 2016).

While only about 50 cases were confirmed, based on the serum presence of anti-ZIKV antibodies, it is estimated that the Yap-outbreak resulted in 5000 infections within a population of only 6700 (Duffy *et al.*, 2009). Retrospective analysis determined that at the time cases of microcephaly were also expanding within that population, though no record of hospitalization or death was documented from these symptoms (Mlakar *et al.*, 2016). In 2013 and 2014 there was an outbreak of the same illness in French Polynesia where an estimated 32,000 people were assessed for ZIKV infections (Baronti *et al.*, 2014; Besnard *et al.*, 2014; Cao-Lormeau *et al.*, 2016). In addition, a total of 42 people were diagnosed with Guillain-Barré syndrome (GBS), through a study during the outbreak and 41 had anti-ZIKV IgM or IgG (Cao-Lormeau *et al.*, 2016; Petersen *et al.*,

2016). The incidence for GBS was far higher than previously described for this very rare neurological disease. This was the first report for a neurological disorder likely linked to infection with ZIKV and was later attributed to abnormal host-directed immune responses resulting from the ZIKV infection (Ritter *et al.*, 2017).

ZIKV continued its progression eastward across the Pacific Ocean as outbreaks were reported in other Pacific Islands including New Caledonia, Easter Island, Cook Islands (2014), Samoa (2015) and American Samoa (2016). Sporadic cases continued to be reported in South-East Asia as well (Thailand, East Malaysia, Cambodia, the Philippians and Indonesia) (Dupont-Rouzeyrol *et al.*, 2015; Roth *et al.*, 2014; Tognarelli *et al.*, 2016; Weaver *et al.*, 2016). ZIKV made landfall in South America around the same time as these outbreaks, the first non-imported cases were reported in Brazil in June 2015 (Zanluca *et al.*, 2015). By December of 2015 there were an estimated 1.3 million suspected cases worldwide since the beginning of the 2007 Yap outbreak (Faria *et al.*, 2016; Hennessey *et al.*, 2016).

While ZIKV local outbreaks were large in respect to the slight population on the island nations of the Pacific, its epidemiology gained statistical robustness in Brazil. Although most reports continued to be characteristic of mild illness, the large population of immunologically naive individuals and the fast spread of the Brazilian ZIKV epidemics allowed clinicians to observe an alarming link to what became the most notorious pathology associated with ZIKV infection – microcephaly. Microcephaly is a condition characteristic of a small head, reduced brain size and impaired cognitive development in newborns usually caused defects in neural development (Salvo *et al.*, 2018). Other less common fetal abnormalities and spontaneous abortions were also reported as associated with ZIKV infections as the epidemic spread from Brazil to other parts of the Americas (including the southern US) and the Caribbean Islands (Faria *et al.*, 2016; Schuler-

Faccini *et al.*, 2016). As of February 2018, a total of 86 countries have reported mosquito borne ZIKV transmission (Center For Disease Control, 2018).

Though fewer cases have been reported in recent days, RNA viruses are subject to faster evolution rates than DNA viruses, due to the fact that they lack proofreading activity (Elena and Sanjuán, 2005). It is likely that Zika will continue to be involved in intermittent cases. Due to past infection patterns and the reputation concerning the change in virulence patterns of RNA viruses, it is possible that it could reemerge as an epidemic if prophylactic treatments are not created (Monath, 2018).

*1.2 Zika Virus Transmission*

The most common recorded means of transmission of ZIKV is through mosquito insect bite. *Aedes* mosquitoes have been identified as the main genus of transmission, primarily *Aedes aegypti* and *Aedes albopictus* (Grard *et al.*, 2014). It is thought *A. aegypti* has high vectoral capacity, the capacity for a vector to transmit disease by a vector to a host, since its primary feeding source is humans and the species often will bite multiple humans in a single meal (Gubler, 2002). Both mosquitoes generally feed during the daytime (Ponlawat and Harrington, 2009). This allows them to access the largest possible blood supply, as most people are active during the day. Consequently, a large number of people have the potential to become infected if bite by an infected mosquito.

Transmission through semen has been reported as well (Araujo *et al.*, 2016; Dai *et al.*, 2016; Mansuy *et al.*, 2016). Viral particles in addition to viral RNA was detected in sperm samples up to 62 days after onset of ZIKV febrile symptoms (Mansuy *et al.*, 2016). Studies have also shown detectable ZIKV RNA in vaginal secretions but there have been no reports on whether the sexual partner of these patients contracted ZIKV or not. ZIKV has also been detected in urine, breast milk, fetal amniotic fluid and saliva of patients positive for infection (Paz-Bailey *et al.*, 2017). However, there is little evidence of

transmission of the virus through any of these fluids. There is a single report of transmission of ZIKV through saliva, in which a ZIKV infected monkey bite a man who later developed ZIKV upon medical diagnosis (Leung *et al.*, 2015). As usual with blood-borne infections, contaminated blood transfusion is also a potential risk that can be minimized by screening for ZIKV and avoiding donations from people who recently traveled to areas where ZIKV has become endemic (Musso *et al.*, 2014).

By far the biggest concern regarding ZIKV infection is its transmission from an infected mother to a fetus. There is likely greater vulnerability in the early stages of pregnancy since the fetus is developing its neural cells. There is evidence a fetus might never develop birth deficiencies by a ZIKV infected mother if the mother contracts the virus during the third trimester of pregnancy (Sotelo *et al.*, 2017). Maternal ZIKV infection had also been shown to manifest differently than in subjects who are not pregnant, primarily, the mother's length of symptoms was prolonged in comparison to individuals who were not pregnant (Nguyen *et al.*, 2017). There is no evidence that previous infection with ZIKV will affect future pregnancies once the virus is cleared from a patients system (Rasmussen *et al.*, 2016).

*1.3 Symptoms of Zika Virus Contraction*

The incubation time of ZIKV is generally anywhere from 3-14 days (Krow-Lucal *et al.*, 2017). Most ZIKV infections present asymptomatically, making ZIKV tests necessary if a pregnant mother has been bitten by a mosquito in a country where ZIKV outbreak is current and prevalent. However, when symptoms are present, they can include some or all of the following: fever, sweating, chills, rash, headache, vomiting, and conjunctivitis (joint and muscle pain). Other, less frequently-reported symptoms include dull hearing, hand and ankle swelling, and subcutaneous bleeding. All previously listed symptoms do not last generally more than a week. Though there have been recorded

deaths from ZIKV, it extremely unlikely that a patient will die from contraction of ZIKV (Petersen *et al.*, 2016).

Neurological complications in adults after contraction of ZIKV has been reported in rare cases, in addition to GBS, paranesthesia as well as muscle weakness that does not progress to GBS is on record (Oehler *et al.*, 2014). GBS itself can hinder movement sensation or organ function and can eventually lead to flaccid paralysis which is usually not permanent. Both the Peripheral Nervous System and the Autonomic Nervous System can be affected, and symptoms can progress to final stages in as little as 3-6 weeks post infection. Proposed mechanisms for how this might occur include Acute Inflammatory Demyelinating Polyneuropathy, which involves activation of the complement system and T cells which in turn activate macrophages and damage myelin. Another proposed mechanism involves production of IgG antibodies and complement against the axolemma (Magira *et al.*, 2003). ZIKV crosses the blood brain barrier (BBB) and infects neural progenitor cells (Li *et al.*, 2016). When these cells are infected it is proposed by researchers that epitope spreading as well as molecular mimicry can cause the previously listed mechanisms to begin (Hadden and Gregson, 2001). Nerves can remyelinate themselves within 6-12 months and patients can recover fully (Yuki, 2015). Other extremely rare neurological cases that have been documented in adults in correlation with ZIKV are Meningoencephalitis and Acute myelitis; though ZIKV has been determined neurotropic, no causative studies have been done on Meningoencephalitis and Acute myelitis (Araujo *et al.*, 2016).

Though the exact mechanism by which ZIKV leads to neurodevelopmental pathologies in the embryo or fetus and to microcephaly is not resolute, several possible mechanisms have been proposed. According to one proposal, ZIKV triggers endoplasmic reticulum (ER) stress and unfolded protein responses as was shown in both *ex-vivo*

cultured neural stem cells (Laguesse *et al.*, 2015) and *in-vivo* within the cerebral cortex of the fetus (Laguesse *et al.*, 2015). The ER stress causes errors in an unfolded protein response in cortical progenitors, these progenitors normally allow for development of projection neurons (neurons which govern neurogenesis). Therefore, progenitors infected with ZIKV will produce fewer projection neurons and will finally settle in the cerebral cortex, leading to apoptosis of those cells, an overall reduction in neurogenesis and a consequential smaller than average brain in the ZIKV infected fetus (Gladwyn-Ng *et al.*, 2018).

Reduced growth occurs in many cases as overall size of ZIKV infected fetuses are smaller than normal when they are born. Many of these newborns also experience hearing loss, vision problems and feeding problems. All these symptoms are due to a lack of development in areas of the brain due to neural cell death and can manifest differently in each case (Acosta-Reyes *et al.*, 2017; Cugola *et al.*, 2016). Still births have also been reported in ZIKV infected pregnant women, though non-ZIKV etiology should not be ruled out in these reports since this evidence is still only correlative (Goncé *et al.*, 2018).

*1.4 Molecular Biology of Zika Virus and Protein Makeup*

Flaviviruses are icosahedral and lipid enveloped. Mature viral *Flaviviridae* are approximately 500 Å and are smaller than immature viral particles which are approximately 600 Å in diameter (Hasan *et al.*, 2018). ZIKV contains a single stranded positive sense RNA genome that is 10,600 bp long and consists of one long open reading frame that encodes a single polyprotein, primarily anchored in the ER by membrane spanning transmembrane helices as depicted below in Figure 1.

The polyprotein is cleaved by cellular and ZIKV produced proteases while some of the products are later glycosylated by glycosyltransferases. There are three main structural proteins (the Capsid or C protein, the membrane or M protein [cleaved from

the prM protein] and the Envelope or E protein) and seven nonstructural proteins (NS1, NS2A, NS2B, NS3, NS4A, NS4B, NS5), each of which contribute to the formation of mature ZIKV particles (Davidson, 2009; Hasan *et al.*, 2018). The genome is packaged within a lipid bilayer surrounded by approximately 180 copies of both the envelope (E) and the membrane (M) glycoproteins. The capsid (C) protein is composed of 100 amino acids and takes part in packaging the viral genome as well as formation of the nucleocapsid core (Hasan *et al.*, 2018).

Glycoproteins prM and E have two transmembrane domains each and are approximately 165 and 495 amino acids respectively (Kuhn *et al.*, 2002). It is thought the prM protein functions as a chaperone to help folding and assembly of the E protein during a cleavage event that occurs post trans-Golgi processing where the Pr is separated from the M protein (Lorenz *et al.*, 2002). After this event, the Pr protein is no longer a part of the mature virion and only the C, M and E proteins remain. E proteins also encompass at least one receptor binding site and a fusion peptide (Hasan *et al.*, 2018).

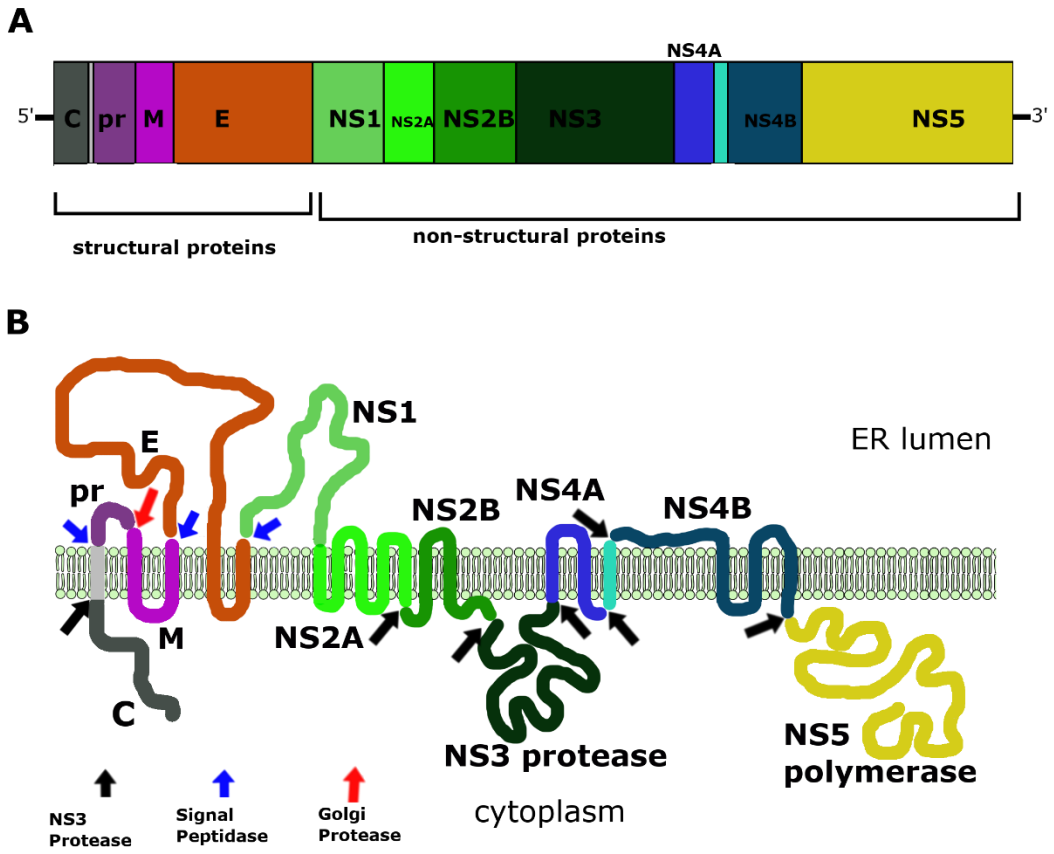


**Figure 1: Components of ZIKV Polyprotein (A) Representation of the ZIKV gene containing the sequences for the structural and non-structural proteins in order (B) Representation of the ZIKV polyprotein embedded in the ER membrane. The cleavage sites are identified by arrows whose etiology are distinguished by color.**

The structures of the ZIKV virion as well as the structure of the C, M and E proteins were resolved at high resolution (Kostyuchenko *et al.*, 2016; Sirohi *et al.*, 2016) and were found to closely resemble the corresponding structures of DENV. The major difference is found in the region that flanks the glycosylation site on the ZIKV E protein (Asn 154 in ZIKV and Asn 153 in DENV) where glycosylation occurs. Glycosylation at the Asn 154 site in West-Nile Virus, another flavivirus, was linked to neurotropism suggesting that it may play a similar role in ZIKV and may be responsible for its neurotropism (Beasley *et al.*, 2005). There exist glycosylation sites (N-,O- and C- linked)

in all ZIKV strains. N- linked glycosylation contributes to multiple functions such as proteolytic processing, protein trafficking and receptor binding (Vigerust and Shepherd, 2007). O-linked glycosylation take part in virus/bacteria-host interaction, ligand recognition and signal transduction (Steen *et al.*, 1998). C-linked glycosylation is thought to play a role in secretion and enzymatic activity (GOTO *et al.*, 2014). N-linked glycosylation was found at Asn-154 in the envelope. O-linked glycosylation was found in positions (7, 47, 48, 170, 173) of the envelope and positions (6, 8, 56) of the membrane protein. C-mannosylation was found only in position 115 of the membrane protein. This makes a total of six glycosylation sites in the ZIKV envelope and four in the ZIKV membrane protein (Gupta *et al.*, 2016).

All *Flavivirus* precursor proteins also hold seven non-structural (NS) proteins. These proteins are NS1, which is involved in replication of RNA as well as assembly of the viral particle and when secreted as a hexamer plays a role in immune evasion (Hasan *et al.*, 2018; Rastogi *et al.*, 2016), NSA2A, which takes part in immune evasion and RNA replication, NS2B, which acts as a cofactor to NS3, NS3, which acts a s major viral protease of the polyprotein (as indicated in Figure 1), NS4A, which acts as a cofactor for NS3, NS4B which also takes part in immune evasion and RNA replication, and NS5 which functions in RNA synthesis and modification. All are essential for replication of the virus particle (Davidson, 2009; Hasan *et al.*, 2018; Murray *et al.*, 2008).

Massive conformational changes occur in virus structure during maturation of the viral particle, host-cell recognition and fusion to the host cell. These changes can be triggered by both PH and temperature, depending on the developmental stage of the particle (Fibriansah *et al.*, 2013). Research on components used for viral replication as well as information concerning conformational changes ZIKV undergoes can be valuable in development of anti-viral compounds which can be administered post-viral infection.

ZIKV and other flaviviruses enter a host through what is known as receptor mediated endocytosis (Hasan *et al.*, 2018). When the virus is inside of the endosome irreversible trimerization of the E protein will be triggered by exposure to the acidic environment of the organelle. Trimerization results in fusion of viral and endosomal membranes (Harrison, 2008). Next, the viral RNA genome is released into the cytoplasm of the host cell and the positive sense RNA is immediately translated into the polyprotein (Figure 1) which includes both non-structural and structural proteins in an effort to yield replication proteins. A double stranded RNA genome is synthesized from the genomic strands of single stranded RNA. This allows for transcription and replication of the genome, creating new viral mRNAs and ssRNA genomes. Particle assembly occurs at the ER, as virions bud and are transported to the Golgi. It is likely that the receptor for ZIKV is the Gas6-AXL tyrosine receptor complex. The Gas6 protein can be found mostly in brain, muscles and male reproductive tissues while the AXL tyrosine kinase is expressed mainly in muscles and male reproductive tissues (Harrison, 2008; Richard *et al.*, 2017). Lower amounts of Gas6 and AXL tyrosine kinase have been described in female reproductive tissues and importantly in the placenta as well (Uhlén *et al.*, 2015).

Immature flavivirus particles form in the ER lumen and are composed of uncleaved prM, and E in the lipid membrane and C. It is important to note that these particles alone are unable to infect a host cell because they do not contain the RNA genome however, any of these structural proteins likely can initiate an immune response (Kaufmann *et al.*, 2009). After viral assembly, immature virions transport out of the ER, to the trans-Golgi network (TGN), then to the cell surface. During this transit, particles undergo protease and pH dependent maturation (Li *et al.*, 2008). The prM protein is cleaved by furin proteases (in humans), producing a glycosylated N-terminal pr fragment which separates completely from the other proteins while the membrane (M) portion

remains anchored to the mature virion. Cleavage and dissociation of the pr peptides from a virion primes viral particles once they infect another cell to undergo low-pH fusion events during cell entry (Harrison, 2008). Though proteolytic processing of prM is essential for viral fusion to host cells, complete maturation of all 60 trimeric spikes is not mandatory for infectivity or fusion (Plevka *et al.*, 2011). Though the mature virions and immature virions share some similarity there are many differences that allow varied functions of each.

In a mature flavivirus, the E protein forms a dimer. Each E protein monomer is composed of three domains: the first domain is the amino terminal domain (DI), which is centrally located in the protein monomer, the dimerization domain (DII) contains the fusion peptide and the carboxy-terminal immunoglobulin domain (DIII). A total of 90 E protein dimers, composed of a total 180 protein monomers, form the smooth surface of the mature flavivirus (Kuhn *et al.*, 2002). The lipid bilayer is mostly unexposed since the E dimers are in a close-packed arrangement which is why a conformational change is required before fusion with the host cell (Hasan *et al.*, 2018; Kuhn *et al.*, 2002). The transmembrane domains from the E and M proteins create antiparallel helices. The two helices in the E protein stem region are amphipathic and lie flat on the viral membrane to interact with the lipid heads of the outer leaflet of the lipid bilayer. The M protein is also helical and an antiparallel coiled-coil (W. Zhang *et al.*, 2003).

Immature flavivirus particles are able to be produced upon addition of $NH_4Cl$ or another base to the growth medium during the final maturation phase because this prevents pH driven prM-E rearrangement (Heinz *et al.*, 1994). Immature viral particles have only 60 trimeric surface spikes and are larger than mature virions (~600 Å). Rearrangement of E and prM proteins occurs in the low-pH environment of the Trans-Golgi Network (TGN) which drives cleavage of the pr peptide from the prM to generate

the mature virus. During this period, the conformation of the immature viral particle changes from 60 E trimers to 90 E dimers. In addition, the angle hinge among DI and DII in each E protein changes by 27 degrees while the E and M anchor regions are also reorganized. The cleaved pr peptide is released as the protein gets secreted to the extracellular environment which is typically slightly above neutral pH (Yu *et al.*, 2009). The process reverses itself when the virus infects a new host cell. Upon endocytosis, the low pH in the endosome causes parallel flat E dimers to disassociate into monomers which then re-associate into trimers. These E protein trimers have three-fold symmetry and employ class II fusion (a classification of viral fusion proteins that require proteolytic processing to create a fusion competent protein, are parallel with respect to the viral membrane, utilize beta sheets as their major secondary structure, and have dimers as their structure of the native fusion protein) (White *et al.*, 2008). In flaviviruses the fusion peptide creates a loop at the end of the E DII. Upon acidification DII inserts itself into the host endosomal membrane. When the lipid membranes of the virus and the cell fuse, the stem region of E fixes itself to a groove on the side of the DII (Y. Zhang *et al.*, 2003).

*1.5 Current Vaccines for ZIKV Infection*

During the most recent ZIKV outbreaks there were no preventative medical treatments available. Spread of disease has been recently prevented by avoidance of travel to areas where outbreaks were occurring (Benelli and Mehlhorn, 2016). Recently, there have been more specific developments in ZIKV prevention, mainly in the realm of vaccine research.

Though there is no approved vaccine for ZIKV, there are some currently in phase 1 clinical trials (Abbink *et al.*, 2018). Most recent attempts at a ZIKV vaccine involve DNA vaccines (Tebas *et al.*, 2017), mRNA vaccines (Pardi *et al.*, 2017; Richner *et al.*,

2017), Purified Inactivated Virus (PIV) vaccines (Modjarrad *et al.*, 2018) and viral vector-based vaccines (Combredet *et al.*, 2003; Lauer *et al.*, 2017; Milligan *et al.*, 2016; Ura *et al.*, 2014; ZIKAVAX). Many of these have been shown to display full protection against ZIKV challenge in mice and rhesus macaques. There are currently 13 open clinical trials testing the previously listed platforms (Abbink *et al.*, 2018).

DNA vaccines are composed of a plasmid which contains a promoter as well as a transgene under control of that promoter. The first assessment of a ZIKV DNA vaccine was done by GeneOne Life Science and Inovio Pharmaceuticals. The DNA vaccine expressed both the Zika pre-membrane (prM) and Envelope (E) genes. Mice in this trial received a priming dose as well as two boosters. There were no severe reactions to the vaccine and it was found to have produced dose-dependent responses when tested 2 weeks after the last administration in mice (Tebas *et al.*, 2017). Challenge experiments were conducted in the interferon receptor knockout mouse model. Serum obtained from vaccinated animals was transfused into nave model animals which were then challenged by a lethal dose of ZIKV with a 92% survival rate (Aliota *et al.*, 2016).

Two DNA vaccines were then modeled for human trials. One was designed to express the ZIKV prM-E proteins as well as a Japanese Encephalitis Virus (JEV) stem region, to increase subviral particle formation. The second was created to produce wildtype ZIKV prM-E. In both vaccine trials, volunteers were administered with three doses. Both were tolerated well, the vaccine without the JEV stem region had higher immunogenicity and is in phase II clinical trials (Abbink *et al.*, 2018; Marques and Burke, 2018).

There are also three candidate vaccines, all created in different research laboratories, based on a purified formalin-inactivated Zika virus (referred to as ZPIV) in Phase 1 clinical trials. Upon combined interim analysis, vaccines were shown to elicit

neutralizing antibodies in all participants with a peak after the second dose for 95% of participants while the other 5% had peak levels during another unspecified portion of the trial. These results also showed protection against ZIKV challenge in 41 of 50 Balb/c mice. Another phase 1 trial studying dose escalation is to be started soon (Abbink *et al.*, 2018).

mRNA vaccines encode a gene of interest (Abbink *et al.*, 2018; Brito *et al.*, 2015). Once it has entered the cytoplasm, mRNA is translated into protein. The most efficient Zika mRNA vaccine contains prM-E mRNA encapsulated by a lipid nanoparticle (Reichmuth *et al.*, 2016). The nanoparticle allows for delivery and stability of the mRNA (Reichmuth *et al.*, 2016). Immunization using this vaccine in both mice and monkeys has induced high levels of neutralizing antibodies against ZIKV (Pardi *et al.*, 2017)When pregnant mice were immunized, the vaccines also prevented fetal injury (Richner *et al.*, 2017). The first phase I/II clinical trial by Moderna Therapeutics is ongoing to determine safety and dose-dependent immunogenicity (Pardi *et al.*, 2017; Richner *et al.*, 2017). While apparently effective, mRNA vaccines require high dose of the immunogen. Moreover, the lability of mRNA makes such vaccines not sufficiently stable at ambient temperatures, constituting a major drawback when considering transportation and distribution of the vaccine in rural areas of the tropics.

Vector based vaccines are made up of a viral vector with a genetically engineered gene that produces a recombinant protein of interest. A modified schwarz stain of measles virus vector vaccine against ZIKV has been developed by Themis Bioscience GmbH and is in phase I clinical trials. It was designed to express the ZIKV prM-E and was tested for immunogenicity in both mice and in monkeys. The current clinical trial aims to assess safety of both high and low doses when given in singular and duplicate

administrations; however no results on this trial have been determined yet (Barouch *et al.*, 2013).

*1.6 Immune Response to ZIKV*

There are many cellular receptors that have been proposed as potential entry receptors for the virus. ZIKV prefers to attack neuronal cells making the Gas6-AXL receptor the most likely candidate (Harrison, 2008). Among other candidates are: dendritic cell specific receptors, ICAM-3 grabbing non-integrin, hepatitis A virus cellular receptor 1 and tyrosine protein kinase 1 (Hamel *et al.*, 2015; Meertens *et al.*, 2017).

Cellular infection with ZIKV encompasses expression of Toll-like 3 receptor (TLR3), retinoic acid inducible gene 1 (RIG-1) and melanoma differentiation associated gene 5. It also causes the upregulation of type 1 and type 2 interferons as well as the upregulation of interferon stimulating gens that mediate antiviral responses (Hamel *et al.*, 2015). Though innate immune mechanisms like TLR3 and MDA5 recognize dsRNA they recognize ZIKV, a positive sense single stranded RNA virus, because although the positive sense strand can be directly translated, ZIKV must create a negative sense RNA intermediate before it can make more positive sense strands to be used as genomes for future virus particles. As a result, the body recognizes both its primary positive sense strand and its negative sense RNA strand as dsRNA and mounts an innate immune response to dsRNA rather than ssRNA (Ball, 1994).

Increase in the expression of TLR3 eventually will cause upregulation of Type 1 interferon (type 1 IFN) (Uematsu and Akira, 2007). Type 1 IFN can stimulate both NK cells and macrophages to elicit an antiviral response. This will cause degradation of RNA as well as necroptosis and apoptosis (Madera *et al.*, 2016). Type 1 IFN, when released, acts on neighboring cells to increase surveillance. The Type 1 IFN will be released from the cell and will bind to the Type 1 IFN receptor on the neighboring cell which will

phosphorylate Signal transducer and activator of transcription 1 and 2 (STAT 1 and 2) which signals through IRF9 to upregulate 2'-5'-oligoadenylate synthase (2'5' OAS) and the protein kinase receptor (PKR). 2'5' OAS uses ATP to become 2'-5'-oligoadenylate (2'5' OA) which causes expression of RNaseL which causes degradation of mRNA and halting of transcription as a result. PKR upregulation causes phosphorylation of Eukaryotic Initiation Factor 2 alpha (elF2 alpha) which shuts down translation and eventually causes apoptosis and necroptosis of the cell (Murphy and Weaver, 2016). Upregulation of RIG-1 ultimately causes an upregulation of Type 1 IFN which results in the same cell death mechanism previously described, it accomplishes this through recognition of the 5' phosphate cap of viral mRNA (Murphy and Weaver, 2016).

Melanoma differentiation associated gene 5 (MDA5) is a RIG-I-like receptor dsRNA helicase enzyme that functions as a pattern recognition receptor (PRR) to recognize dsRNA greater than 2,000bp. It is also believed that MDA5 recognizes higher order RNA structures that form as a product of annealing of complementary RNAs generated during a viral infection (Pichlmair *et al.*, 2009). It is considered a DEAD box protein as it has a conserved motif Asp-Glu-Ala-Asp (DEAD). Both RIG-1 and MDA5 contain two N-terminal caspase recruitment and activation domains (CARDs) as well as a C-terminal regulatory domain which allow for downstream signaling (Kang *et al.*, 2002). Both RIG-1 and MDA5 act on IFNβ promoter stimulator 1 (IPS-1). IPS-1 works in conjunction with TRAF3 which phosphorylates TBK1 which phosphorylate IRF3/7 and causes the release of Type 1 IFN (Kawai *et al.*, 2005).

In addition to the previously described effects of Type 1 IFN release, Type 2 interferon (IFN gamma) is released by activated NK cells and activated T cells. It has been shown that ZIKV infected cells have upregulated amounts of IFN gamma (Hamel *et*

*al.*, 2015). Such a situation indicates possible activation of NK cells and T cells in addition to previously described immune mechanisms (Murphy and Weaver, 2016).

Beyond innate immune responses, preliminary reports indicate that neutralizing antibodies (usually to E protein) were produced as seen in many other flavivirus infections (Dai *et al.*, 2016). There exists significant cross reactivity between ZIKV and other flaviviruses, generally to what are believed to be conserved epitopes. This situation has made it difficult to determine ZIKV infection by utilization of antibody titer in areas where people have previously been infected with other flaviviruses like Dengue. Dengue virus (DENV) is the most common mosquito-transmitted human flavivirus and since there is much similarity between DENV and ZIKV, there is also much antigenic overlap. This has resulted in antibody-dependent enhancement (ADE), where anti-DENV antibodies and antibodies against other flaviviruses increase the infectivity of ZIKV (Paul *et al.*, 2016). Several proposed mechanism have been researched to explain why this occurs. It is possible the viral surface proteins are fastened with antibodies against a virus of one stereotype that binds to a similar virus of a different stereotype, in this case an antibody against DENV might bind to ZIKV. The binding is primarily supposed to neutralize the virus and keep it from attaching to the cell, instead, the antibody that binds to the virus also binds to the Fc- region antibody receptor (FcγR). As a result the virus is brought into close juxtaposition and the cell internalizes the virus through a normal infection route (Takada and Kawaoka, 2003).

In addition, an antibody to a virus meant to neutralize DENV might not neutralize ZIKV, instead, the virus is injected into the cell as a virus particle after it is sub-neutralized by the antibodies against DENV. When the virus is phagocytosed as an antigen-antibody complex, it is then degraded by macrophages. The antibodies no longer

sub-neutralize the virus due to acidic conditions of the phagolysosome within the macrophage and the virus will become active within that cell (Halstead, 2003).

Adaptive immune studies on ZIKV have shown that though antibody-dependent enhancement can occur in those previously exposed to other flaviviruses, there is also a chance previous exposure can produce neutralizing antibodies against conserved epitopes and concerns for ADE occur on a case by case basis (Priyamvada *et al.*, 2017).

*1.7 Biology of Virus Like Particles and Immune Effects*

Virus like particles (VLPs) are a class of subunit vaccines that mimic the structure of an actual virus particle. They are generally recognized by the immune system since they present authentic viral epitopes to the immune system (Noad and Roy, 2003). VLPs are formed through self-assembly of an envelope or capsid protein of viruses within a host cell, generally of mammalian origin for most current VLP vaccines (Grgacic and Anderson, 2006). In past studies, patients who were immunized with VLPs were more likely to elicit a dominant Th1 immune response (comprised of IgG2a and IgG2b). They also were able to elicit a larger panel of antigenically specific neutralizing antibodies against viral isolates when compared to subunit vaccines that confined only some of the viral epitopes on the actual virus (Bright *et al.*, 2007). The self-assembly of VLPs occurs in the same way self-assembly of viruses occurs within a cell. The proteins are generally targeted to the area in which the virus normally develops (such as the ER or the plasma membrane) and the particles bud to mimic immature virus particle formation (Gheysen *et al.*, 1989). Often, these particles will be produced in an expression system, and protein analysis will be performed on them to determine that different components are present in conformationally correct ways. This protein analysis can be completed by western blot analysis and utilization of monoclonal or polyclonal antibody preparations specific to the protein of interest (Christensen *et al.*, 1996)

VLPs, like native viral particles, contain relevant epitopes in the proper conformation. Such a circumstance is needed to elicit protective antibody responses (Zabel *et al.*, 2013). The size of the antigen is also a chief factor in determination of how these antigens will gain access to lymphoid organs (Gonzalez *et al.*, 2011). Viral particles usually encompass sizes that are between 20 and 200 nm (Zabel *et al.*, 2013). This size range allows for drainage to lymph nodes as particles that are less than 200 nm in size are brought to subcapsular regions of B cell follicles on the surface of myeloid and B cells (Cinamon *et al.*, 2008). VLPs also are generally between 20-200 nm, making their transport to lymphoid organs efficient (Zabel *et al.*, 2013).

VLPs encompass a highly repetitive structure. This will efficiently crosslink a BCR upon presentation to it which in turn causes potent B cell activation (Bachmann and Zinkernagel, 1997; Zabel *et al.*, 2013). This activation causes B-cell proliferation and upregulation of MHC class II and costimulatory molecules. Activation of B cells allows for formation of both primary foci and germinal centers (GCs). In primary foci, short lived B cell responses are produced, whereas in GCs the B cells can undergo somatic hypermutation (in dark zones of GCs) and affinity maturation (in light zones of GCs)(Murphy and Weaver, 2016). B cells then travel to boundaries between B-cell and T-cell areas contained in secondary lymphoid tissues. In doing this, B cells pass through the mantle zone where T cells display CD40L which interacts with CD40 on activated B cells. Through secretion of cytokines such as IL-4, IL-5, and IL-6, full B cell activation can occur, and cells will re-enter the dark zones. These cells will exit as memory B cells or long-lived plasma cells with allow for adaptive immune memory responses (long lived host immunity to presented antigen)(Murphy and Weaver, 2016; Zabel *et al.*, 2013). The repetitiveness of these viral particles and VLPs also facilitates complement fixation

which in turn enhances deposition on B cells, further enhancing previously described B cell activation and adaptive host immunity (Carter and Fearon, 1992; Zabel *et al.*, 2013).

Testing of the immune response to VLPs is like that of most other vaccine platforms. Dose dependent immunization should occur to determine the amount needed to create a sufficient neutralizing immune response. In addition, dose dependent studies should be performed in conjunction with intermittent immunization studies to determine if boosters are required for a vaccine platform to create a sufficient immune response. Antibody titers in response to the vaccine can be measured by means of an enzyme-linked immunosorbent assay (ELISA) both after immunization and after viral challenge (Bertolotti-Ciarlet *et al.*, 2003)

*1.8 Components of Bean Yellow Dwarf Virus Expression Vector*

Geminiviruses, like BeYDV, have DNA genomes able to duplicate in high-copy number. This ensues because replication occurs by a rolling circle mechanism that functions through a double-stranded intermediate. In addition, this intermediate acts as a template for viral open reading frame (ORF) transcription (Mor *et al.*, 2003). Such a system allows for speedy production of a particular protein of interest and for this reason, was chosen for use in this study. The system used in the proposed expression vector utilizes an improved geminiviral vector system that contains three separate expressions of protein on a single cassette. The first segment that expresses a protein contains a 35S cauliflower mosaic virus protomer. Regulation of transcription requires *cis* elements like this one in order to express corresponding trans-acting proteins (Benfey and Chua, 1990). The 35S promoter is followed by a P19 RNAi suppressor that originates from tomato bushy stunt virus. This 19kDa protein forms dimers that bind to short interfering RNAs (siRNA) in an effort to express RNA silencing mechanisms that might be used by the plant to inhibit expression of the cassette (Hsieh *et al.*, 2009). Following

P19 is protease inhibitor 2 (Pin2) which mediates polyadenylation of the first expression, the polyadenylation allows for formation of mature mRNA so that translation can occur from it (Diamos and Mason, 2018).

The second expression cassette is mostly specific to the expression in this study. It contains a Long Intragenic Repeat (LIR) which contains a bidirectional promoter to express native genes. These are noncoding regions that contain sequences capable of forming a hairpin structure and they contain a conserved 9-base sequence that is found in all geminiviruses. LIRs are necessary for initiation of rolling circle replication as well as synthesis of the complementary start (Mor *et al.*, 2003). There is also a P35s viral promoter is repeated twice. This promoter was taken from cauliflower mosaic virus and it increases the frequency of transcription initiation (Mor *et al.*, 2003). Following the promoter is the Barley alpha amylase Signal Peptide (BASP) which targets the protein immediately followed by the BASP to the ER for correct formation and processing, a mechanism most like the actual ZIKV (Mukhopadhyay *et al.*, 2005). Following the BASP are DNA sequences that produce the native ZIKV proteins, the pr, M, and E. The Zika pr is required during processing of immature viral particles to mature viral particles and should be separated from the M protein through cleavage by a furin-like protease. The M protein forms the membrane of the particle and it is attached to the envelope of the fully formed Zika VLP. Finally, the E protein forms the envelop which generally initiates the most immunogenicity upon immune stimulation. The Ext3 allows for the placement of a poly A tail at the end of the transcribed DNA strand. Finally, the matrix attachment region signals to bind to the nuclear matrix to promote stability post-transcription and causes the vector to look more like a segment of chromosomal DNA (Mor *et al.*, 2003). This is meant to enhance the expression and transcription of the gene of interest (Phi-Van *et al.*, 1990).

Finally, the third expression also begins with LIRs which have a bidirectional promoter to express native genes. It is followed by C1 and C2. These both encode the *rep* and *repA* proteins. Thought these are two separate genes they can undergo a splicing event which can splice the two genes together. If the splicing does occur, then only the *rep* protein is produced. If no splicing occurs, then *repA* is produced. The splicing event will occur only about half of the time, though both are needed to amplify the DNA. *RepA* conditions the nucleus to be favorable for the replication of DNA. This maintains DNA synthesis and allows the cell cycle to remain in S phase because it binds to retinoblastoma protein. *Rep* also has a consensus sequence that allows for binding to retinoblastoma protein to make the cell stay in the S phase of the cell cycle. The Short intergenic region (SIR) contains a polyadenylation element for the genes before it (Mor *et al.*, 2003).

Other components of the Gemini vector that are not translated include colE1 ori which is the origin of replication for DH5 alpha cells (*Eshceria coli*). The KanR gene allows for the gene to be resistance to kanamycin. TrfA makes a *trif* protein that will bind to the origin of replication for agrobacterium and allow replication to ensure and RK2 oriv is the origin of replication for agrobacterium (Becker *et al.*, 1992). In conjunction with one another, these components of the expression cassette allow for speedy production of the protein of interest.

*1.9 Agroinfiltration*

Agroinfiltration provides a low-cost, scalable, safe and quick means of protein production. Such a production platform is preferable for viruses such as ZIKV, where many of the countries hit hardest by the virus do not have easy access to healthcare or excess currency to spend on medicine to treat the virus and symptoms resulting from it (United Nations Development Programme, 2017).

Current leading platforms in biopharmaceutical production are mammalian cells, bacteria and yeast, which all carry higher associated production costs in initial laboratory tests than those of plants such as *N. benthamiana* (Evens and Kaitin, 2015). In addition, cells such as mammalian cells take more capital to produce in large quantity than plant-based production methods since plants encompass higher scalability. This scalability is achievable since plants produce their protein on a short timescale (only a few days) while mammalian cells produce a protein of interest on a much larger timescale (weeks) (Fischer *et al.*, 2004).

In addition, there is supplemental safety associated with plant made therapeutics. There exists very low likelihood that plants will carry pathogens harmful to humans. Whereas therapeutics made in mammalian cell lines can become contaminated with pathogens harmful to humans, making plants a safer alternative platform for protein production (Daniell *et al.*, 2009; McCormick *et al.*, 2008)

Through processes such as vacuum infiltration, large quantities of plants are given the ability to transiently express a gene of interest (Chen *et al.*, 2016; Rivera *et al.*, 2012). Large-scale production is preferred when producing therapeutics that must be transported to locations with limited access to medicine and money.

Unlike transgene expression, transient expression platforms do not require integration of transgenes into the host plant genome. Pre-grown plants, once they have undergone agroinfiltration, begin to express the construct of interest in a short time. This process can be accomplished in days as opposed to weeks with transgene expression allowing for quick access to needed therapeutics (Krenek *et al.*, 2015). Quick access to these therapeutics is key in cases where treatment must be created and distributed quickly such as outbreaks like the ones witnessed involving ZIKV.

Such a method utilizes *Agrobacterium tumefaciens*. This method was initially developed by Kapila *et al*. in 1997 in which a suspension of recombinant *A. tumefaciens* was infiltrated into tobacco plants (Kapila *et al*., 1997). The method was successful because the *A. tumefaciens* enables transfer of transfer DNA (T-DNA) to most of the leaf cells, allowing them to express transgenes at high levels without a requirement for transformation of the entire tobacco plant (Matsuo *et al*., 2016). The complex extrachromosomal T-DNA structures form in the agrobacterium-infiltrated plants directly after the leaves are transfected (Yang *et al*., 2018). The T-DNA normally allows for the synthesis of enzymes auxin and cytokinin which enables the plant to uncontrollably grow. When used in a biotechnology setting, the opine-synthesis genes are removed from the T-DNA and replaced with a gene of interest (Lee and Gelvin, 2008). Agrobacterium can transfer foreign DNA into both monocotyledons and dicotyledonous plants by hijacking host factors and cellular processes then by carrying out multiple interactions with host-plant factors (Lacroix and Citovsky, 2013).

### *1.10 Study aim*

The aim of this project was to express the Zika prM and E proteins in *Nicotiana benthamiana* plants with the hypothesis that Zika Virus-Like Particles will self-assemble within the plant. A Gemini viral expression system was utilized and allowed for quick and affordable production of the protein. After verification through western blot analysis, the proteins were visualized through Transmission Electron Microscopy to ensure particle formation.

## 2. METHODS

### *2.1 Construction and Cloning of Expression Vector*

Table 1:

Primers Used in This Study

| # | Name of primer | 5' Sequence 3' |
|---|---|---|
| 1 | ZprM-Bsa-F | ggGGTCTCTCgTGGTGCCGAGGTCACTAGAC |
| 2 | M13-RHT | GGAAACAGCTATGACCATG |
| 3 | 35S-F | AATCCCACTATCCTTCGC |
| 4 | BASP-G-BSA-R | gcGGTCTCCACCAGAAGCAAGAGAAGC |

Initially, construction of the expression vector required procurement of three separate vectors. A vector containing the ZIKV prM and E protein (pUC57-ZCME-F) was provided by Lydia Meador. A vector containing the barley alpha amylase signal peptide or BASP (pBYR2eK2M-BAZE) was provided by Andrew Diamos. A geminiviral replicon vector (pBYR2eK2MC-GFP) was provided by Hugh Mason and contained the vector backbone for the proposed construct. The final vector was created from these three initial vectors. Since one DNA segment from each of these constructs was needed, it was imperative to introduce restriction sites shared amongst the segments. PCR was performed on template pUC57-ZCME-F with primers ZprMBsaF and M13RHT (Table 1). This process created a BsaI site (5'-GAGACC-3') so BsaI could cut five base pairs upstream of the site and create a left sticky end. This process also allowed for creation of a Sac I site (5'GAGCTC-3') on the 3' end of the amplified segment. PCR was also performed on the pBYR2eK2M-BAZE with primers 35s-F and BASP-GB-R (Table 1). This process created a Xho I site (5'-CTCGAG-3') on the 5' end of the segment and a BsaI site (5'-GGTCTC-3') on the 3' end of the amplified segment to create a right sticky end,

which would be able to anneal with the BASP segment of DNA. This PCR created a final segment that was ~240 bp.

Next, 30 µL of each PCR was mixed and run on a 1% agarose gel (400 mg agarose, 40 ml TAE, 4 µL cybersafe) at 115 V for 50 minutes. The segments were present at the predicted positions and were excised and purified using GeneClean© Protocol. A total of 8 µL of purified Zika prME PCR segment that originated from pUC57-ZCME-F was digested with BsaI-HF and SacI-HF. A total of 8uL of purified BASP PCR segment that originated from pBYR2eK2M-BAZE was digested with BsaI-HF XhoI. Finally, the pBYR2eK2MC-GFP was digested with SacI-HF and XhoI. The segments were present at the predicted positions and were excised and purified using GeneClean© Protocol.

*2.2 Ligation of Segments*

The purified samples were ligated together by taking 2.83 µL of each purified segment (ZprME, BASP, Gemini vector backbone), 1.0µL of 10x ligase buffer and 0.5 µL of T4 DNA Ligase. After mixing and spinning down for 2 s at 6000 *xg*, the ligation was allowed to react overnight at 16 °C. Ligation precipitation followed, 0.5 uL of glycogen was added to the mix, a 0.5 volume of 7.5 M ammonium acetate. And 1.0 volume (~15.75 µL) of 2-propanol was added to the mixture. The ligation mixture was put on ice for 10 minutes and centrifuged at full speed for 5 minutes. Supernatant was decanted and ~450 µL of 70% ethanol was added and was washed by inversion 4 times. Mixture was spun at 13,000 RCF. Ethanol was decanted, and tube was placed sideways on a 55 °C heating block for 10 minutes. Precipitate was resuspended in 3 µL sterile milli-q water.

For transformation by electroporation, a 40 µL aliquot of electrocompetent DH5α *E. coli* cells was mixed with 1 µL of resuspended ligation product. The mixture was transferred to a dry pre-chilled cuvette and electroporated using an electroporator (voltage, capacitance and resistance settings were 2.5 kV, 25 µF, and 200 Ω,

respectively). Immediately 0.5 mL YENB (0.75% Bacto yeast extract, 0.8% Nutrient Broth, adjust pH to 7.5 with NaOH) was added and cells were transferred into a 1.5 mL tube. They were shaken at 200 rpm for 1 hour then were plated on an LB-agar plate supplemented with kanamycin. Ten colonies that grew on this plate were transferred to another plate and allowed to grow overnight for screening purposes. Overnight-grown colonies were screened to identify transformants by PCR using the primer pairs 35S-F and ZM-Spe-R (expected size ~700 bp), and ZE3-Bam-F and Ext3i-R (expected size ~700 bp). A single positive colony was transferred to YENB media and again incubated overnight at 37 °C. Plasmids were extracted from the media the next day and were subjected to sequencing to verify successful clones. *A. tumefaciens* (strain EHA105) was transformed by electroporation essentially as described above except that the selective growth medium contained kanamycin and rifampicin and was allowed to grow overnight.

*2.3 Agroinfiltration and Expression*

*A. tumefaciens* cells harboring the pBYR2eK2M-ZprME expression vector were grown overnight and were harvested by centrifugation for 10 minutes at 5,000 *xg*. The cultures were resuspended in 5 mL of 1x infiltration (10 mM 2-(N-morpholino) ethanesulfonic acid (MES), 10 mm MgSO4, pH 5.5). Optical density of the culture was read at 600 nm and diluted as needed to $OD_{600}$ = 0.3 in 1× infiltration buffer using the equation $C_1V_1 = C_2V_2$. Culture trials were initially diluted to OD 0.1 in a previous test, but plant expression of proteins failed upon Coomassie staining. The resulting bacterial suspensions were used to infiltrate 6-week-old *N. benthamiana* plants. Infiltration was accomplished by injecting the bacterial suspension into the leaves using a needle-less syringe after making a small puncture in the leaf (Huang *et al.*, 2009). After infiltration was complete, plants were stored in a 25 °C growth chamber for four days until harvest.

*2.4 Small Scale Extraction of Proteins*

Agroinfiltrated-leaf tissue samples were homogenized with an approximately a 1:4 ratio (weight in mg: volume in µL) of extraction buffer. Extraction buffer for the first sample of leaf tissue was PBS (0.0100 M $Na_2HPO_4$, 0.0018 M $KH_2PO_4$, 0.1370 NaCl and 0.0027 KCL pH=7.4) with 0.1 M sodium ascorbate, 1 mM phenylmethylsulfonyl fluoride (PMSF). Where indicated Triton X-100 was added to the specified concentrations.

Approximately 4 samples of 200 mg of infiltrated leaf tissue were placed in their respective 1.7 ml microcentrifuge tube and appropriate amounts of ice cold extraction buffer were added. Half (2) of the samples included tubes that contained infiltrated leaf tissue extracted in the first buffer listed and the other half (2) contained infiltrated leaf tissue extracted in the second buffer listed, which contained Triton-X 100. The same process listed proceeded for 4 un-infiltrated leaf tissue samples to act as a control to compare to the infiltrated leaf tissue samples. Four metal beads were added to each tube and the tubes were placed a bead beater (Next Advanced Bullet Blender 24) for 5 rounds of 2 minutes each. Tubes were placed on ice in between each 2-minute round for 30 seconds. Crude extract was centrifuged at 10,000 *xg* for 10 minutes at room temperature. Supernatant was then separated from the pellet and the pellet was stored at -80 °C separately.

*2.5 Protein Purification Steps for Small Scale Extraction*

Since samples were performed in duplicate, one sample of each preparation (Infiltrated w/ extraction buffer, Infiltrated w/ extraction buffer +1% triton, un-infiltrated w/ extraction buffer, un-infiltrated w/ extraction buffer + 1% triton) was purified by acid preparation to test protein stability. A total of 500 µL of each duplicated sample's supernatant was taken and 16 µL of phosphoric acid was added. The tubes were placed in a 4 °C cold room for 10 minutes on a rotator. Then the samples were taken and

18 µL of NaOH was added to each tube to bring the samples back to equilibrium. Samples were again spun down at 10,000 *xg* for 10 minutes and supernatant was taken and transferred to a new 1.7 ml microcentrifuge tube to be used for SDS-PAGE and western blot analysis.

*2.6 SDS- PAGE and Immunoblotting*

For SDS-PAGE, plant proteins were mixed with 5×.non-reducing sample buffer (3.0 ml glycerol, 1g Sodium Dodecyl Sulfate, 7 ml 4xtris (pH 6.8) at 0.5 M, 1.2 ml bromophenol blue, 2 ml ddH20). The samples were separated on 10% polyacrylamide gels (5 ml of 40% Acrylamide/Bis Solution [AA/BA] 37.5:1, 2.5 ml 3 M Tris PH 8.8, 12.5 ml ddH2O, 1:1000 ammonium persulfate [APS] and 1:10000 N,N,N,N, Tetramethyl-ethylendiamine [TEMED]) at 100 V for 1.5 hours. Gels were then transferred onto polyvinylidene difluoride (PVDF) membrane in ice cold PVDF transfer buffer (100 ml of 10 X transfer buffer [144 g glycine, 30 g tris base= 384 mM Glycine and 50 mM Tris PH to 8.3], 200 mL methanol and 700 ml ddH2O) at 110 V for 18 minutes. PBST (PBS with 0.002% Tween-20) was mixed with a 5:100 (w:v) evaporated milk to create 5% PBSTM. PVDF membranes were blocked in 5 % PBSTM overnight. The next day they were washed with PBST for 5 rounds of 5 minutes each.

Both monoclonal and polyclonal antibody probes were used in this study, post-SDS-PAGE to determine which proteins were present in samples. Monoclonal antibodies detect only a specific epitope on an antigen. As a result, all antibodies applied to the transfer membrane should target the same epitope. The monoclonal antibody used in this study conformationally recognizes the ZIKV envelope domain II-III fusion loop and was provided by Mary Pardhe and Hugh Mason. It only recognizes this epitope if the protein is in the correct shape. As a result, only non-reducing samples will yield positive results when this antibody is utilized. The use of such an antibody ensured the protein

being produced was like the native ZIKV protein and would be likely to initiate an immune response to the actual ZIKV if the patient was exposed to it in the future.

Polyclonal antibodies recognize multiple epitopes on a single peptide. Since these antibodies are produced in animals who also have adaptive immune responses to other peptides, cross reactivity to antigens that the polyclonal antibody preparation might not have been intended for may occur (Hanly *et al*., 1995).

After being washed with PBST, membranes were incubated in a 5 ml solution containing 1% PBSTM and a 1/50 dilution of the monoclonal antibody targeting the Zika E protein domain II-III fusion loop. Membranes were incubated at room temperature (RT) for 2 hours. They were then washed again in PBST for 5 rounds of 5 minutes each and were incubated in a solution containing 1% PBSTM and a 1/5,000 dilution of a secondary goat anti-human HRP linked antibody at RT for 2 hours. The membranes were washed in PBST again for 5 rounds of 5 minutes and were exposed to developing solution (Western Blotting Luminol Reagent 750 µL of Solution A and 750 µL of Solution B, Santa Cruz biotechnology) and were developed to determine protein presence.

*2.7 Time Course to Determine day of Highest E Protein Expression*

A new set of *N. benthamiana* plants was infiltrated, at 2 days post infiltration (DPI) two leaves were taken as samples. Approximately 200 mg of leaf material was taken from the leaves and frozen. This process was repeated for 3, 4, and 5 DPI. Each of the samples were extracted in PBS as described in the small-scale extraction section and aliquots of the soluble fraction were set aside for both reduced and non-reduced samples. After creation of the samples they were run on 10% polyacrylamide gels, were transferred onto PVDF membranes and were incubated using both the monoclonal anti-Zika E antibody and the polyclonal anti-Zika E antibody. After obtaining developments the

images were scanned using ImageJ software and the intensity of the bands present in the ~54 kDa range were determined.

*2.8 Determination of Protein Solubility*

To ensure the detected ZIKV E protein was present in the supernatant rather than the pellet, further solubility determination tests were done following the schematic displayed in Figure 2 below. Small scale extraction took place for a single construct infiltrated leaf tissue sample utilizing PBS extraction buffer. After the extraction was complete the supernatant was set aside, and the pellet was again resuspended in 800 µL of PBS extraction buffer, four metal beads were placed into the sample and it was placed back into the bead beater for 5 rounds of 2 minutes each, sample was placed on ice for 30 seconds in between each 2-minute round. The sample was centrifuged at 10,000 *xg* for 10 minutes and the supernatant was separated from the remaining pellet. This process was repeated using the pellet that resulted from the previous extraction. The pellet was mixed with 800 µL of PBS Extraction buffer that contained 0.1% Triton- X 100. Four metal beads were placed into the sample and it was placed back into the bead beater for 5 rounds of 2 minutes each. The sample was centrifuged at 10,000 *xg* for 10 minutes and the supernatant was separated from the remaining pellet. This process was again repeated using the pellet that resulted from the previous extraction. The pellet was then mixed with 800 µL of PBS extraction buffer that contained 1% Triton-X 100. The supernatant was separated from the pellet, was mixed with non-reducing sample buffer and all samples were ran on a 10% polyacrylamide gel at 100 V for 1.5 hours, transferred to PVDF membranes and probed with the monoclonal anti-Zika E domain II-III fusion loop antibody used previously. The membranes were then developed using methods previously described.

At a later date, the same extraction protocol was followed on a different set of leaf tissue samples that harvested the same way as all samples used in this study and was extracted in PBS. The supernatant samples were then also mixed with reducing sample buffer and were boiled for 5 minutes or were mixed with non-reducing sample buffer. These samples were run on a 10% polyacrylamide gel, transferred to PVDF membranes and probed with either polyclonal anti-Zika E, polyclonal anti-Zika prM or polyclonal anti-Zika M. The first sample set aside in Figure 2 (Supernatant transferred to a new tube after extraction of the pellet in PBS) was not ran on these gels due to lack of space available on the gel.

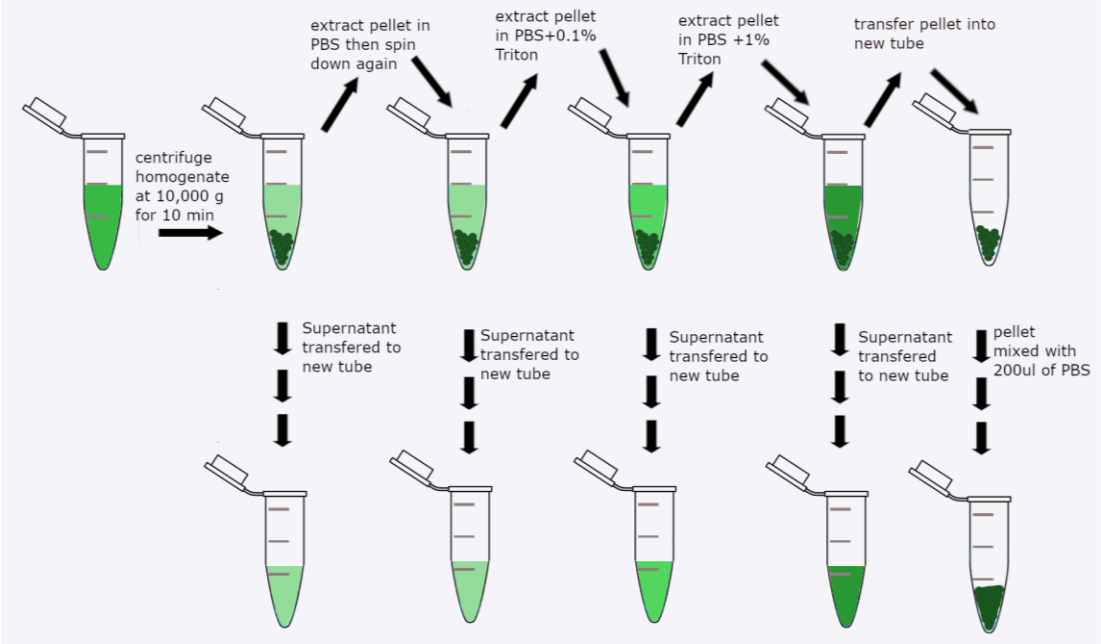


**Figure 2: Schematic Displaying the Sequence of Extractions to Determine Protein Solubility in the Sample.**

*2.9 Large Scale Protein Extraction*

The agroinfiltrated leaf tissues harvested at 4 DPI (20 g), samples were homogenized with an approximately 1:2 ratio (weight in g: volume in ml) of extraction buffer. Extraction buffer for all samples of leaf tissue was PBS extraction buffer. Leaf

tissue and ice-cold extraction buffer were homogenized with the appropriate volume of extraction buffer using a Bullet Blender machine (Next Advance, Averill Park, NY). The homogenized leaf tissue was then placed in a beaker, covered in parafilm and rotated for 30 minutes with a 1.5-inch-long stir bar at 4 °C. The homogenate was centrifuged at 10,000 *xg* for 10 minutes at 4 °C. The supernatant was separated from the pellet and the pellet was stored at -80 °C for further use.

*2.10 Sucrose Gradient*

Primarily, a 10% sucrose gradient (5 g sucrose in 50 mL PBS), a 20% sucrose gradient (10 g sucrose in 50 mL PBS), a 30% sucrose gradient (15 g sucrose in 50 mL PBS), a 40% sucrose gradient (20g sucrose in 50 mL PBS) and a 50% sucrose gradient were created. As seen in Figure 3A, the first gradient that was ran contained 2 ml of 50% sucrose gradient at the bottom of a 15 mL centrifuge tube, 2 ml of 40% sucrose gradient above that layer, followed by 2 ml of 30% sucrose gradient, 2 ml of 20% sucrose gradient, 2 ml of 10% sucrose and 4 ml of supernatant isolated from the homogenate (Fig 3A).

The second sucrose gradient prepared utilized a 20% sucrose gradient and a 70% sucrose gradient. The bottom of the tube contained 2 ml of 70% sucrose, 2 mL of 20% sucrose above that layer and 8 ml of supernatant from the extracted leaves (Fig 3B). Sucrose gradients were centrifuged in an ultracentrifuge with a 28,000 rotor at 28,000 rpm for 2.5 hours. Extracts were carefully taken out of the tubes with a flat tip pipette to ensure accuracy of results when examined by western blot analysis.

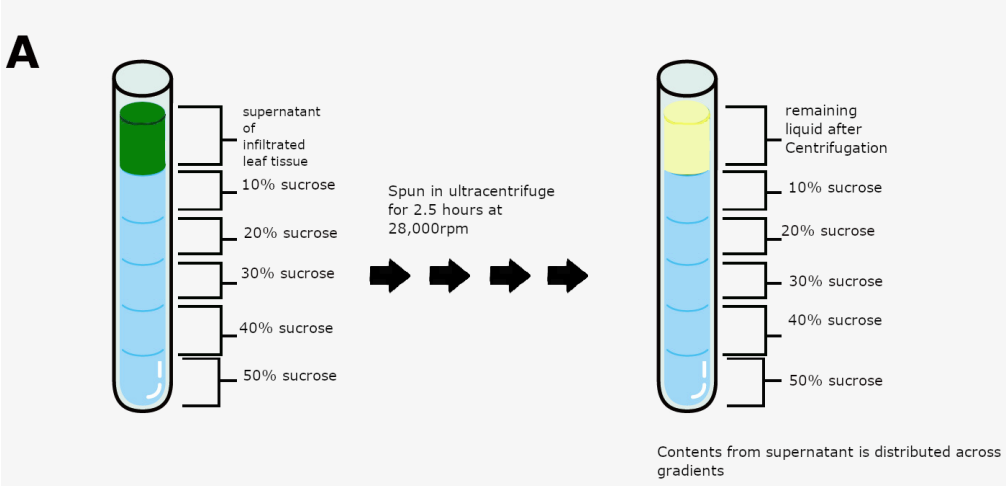


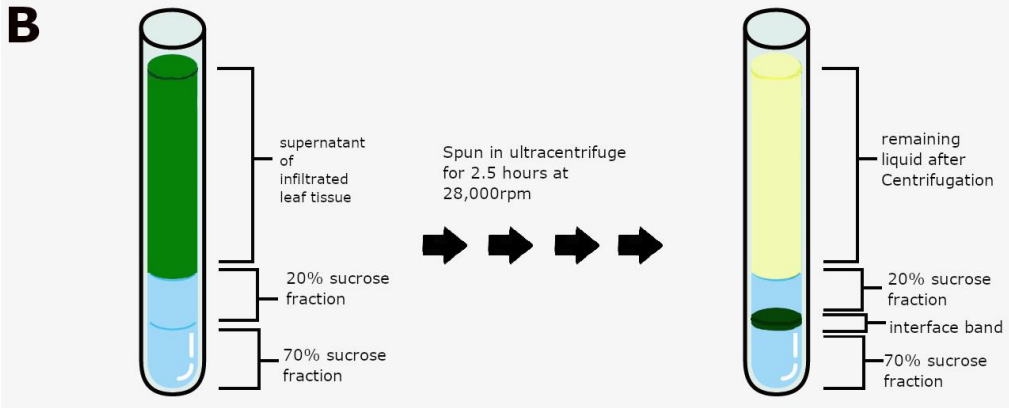


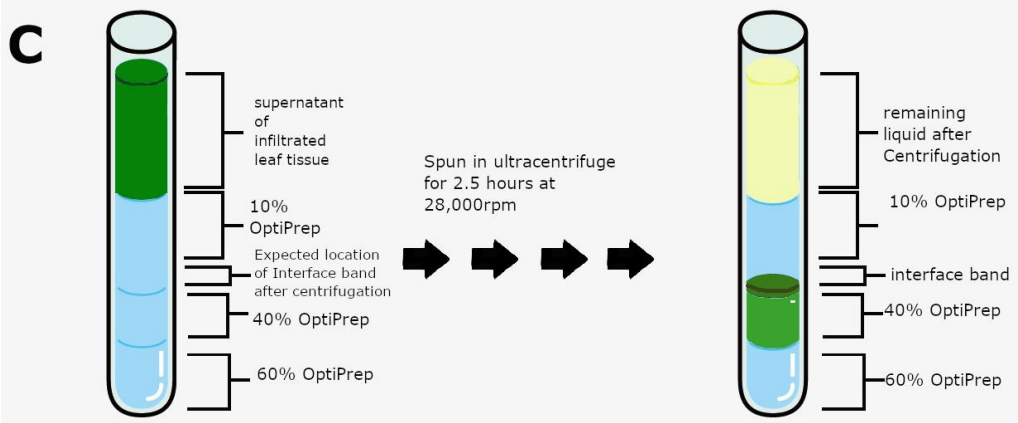


**Figure 3: Schematics of Gradient Setup (A) A sucrose gradient containing 10%, 20%, 30%, 40% and 50% sucrose was made to isolate particle (B) A sucrose gradient containing 20% and 70% sucrose fractions meant to condense the VLPs at an "interface band." (C) An OptiPrep gradient containing 10%, 40%, and 60% gradients meant to condense the VLPs at an "interface band" from viewing under TEM.**

*2.11 Determination of Protein Components Utilizing Different Ab Probes*

Samples taken from the sucrose gradients in Figure 3A and Figure 3B were initially mixed with non-reducing sample buffer and ran on a 10% polyacrylamide gel at 100 V for 1.5 hrs. Gels were then transferred onto PVDF membrane in ice cold PVDF transfer buffer (100 ml [384 mM Glycine and 50 mM Tris PH=8.3], 200 mL methanol and 700 ml ddH2O) at 110 V for 18 minutes. PVDF membranes were blocked in 5% PBSTM solution overnight. The next day they were washed with PBST for 5 rounds of 5 minutes each. Membranes were then incubated in a 5 ml solution containing 1% PBSTM and a 1/1000 dilution of the same monoclonal antibody targeting the Zika E protein domain II-III fusion loop that was used in previous tests, but this aliquot of the antibody was from a different prep than those previously used in the study. The membranes were incubated at RT for 2 hours. The membranes were then washed again in PBST for 5 rounds of 5 minutes each and were then incubated in a solution containing 1% PBSTM and a 1/5,000 dilution of secondary goat anti-human HRP linked antibodies at RT for 2 hours. Membrane was again washed with PBST five times for five minutes each, was doused in developing solution (Western Blotting Luminol Reagent 750 µL of Solution A and 750 µL of Solution B, Santa Cruz biotechnology) was developed to view presence of proteins.

Next, 200 µL aliquots were taken in duplicate from sucrose gradients in Figure 3B after centrifugation. One of the respective samples was mixed with 5x non-reducing sample buffer while the other was mixed with 6x reducing (3.0 ml glycerol, 0.93 g DTT, 1 g SDS, 7 ml 4x tris (pH 6.8) 0.5 M, 1.2 mg bromophenol blue) sample buffer. All samples were ran on a 10% polyacrylamide gel. The sample gel with the same samples and conditions was ran in triplicate for both reducing and non-reducing samples. Gels were then transferred onto PVDF membrane in ice cold PVDF transfer buffer at 110 V for 18

minutes. PVDF membranes were blocked in 5% PBSTM solution overnight. Then washed with 1x PBST for 5 rounds of 5 minutes each. Membranes were each incubated differently. Membranes containing non-reduced samples were incubated in a 5 ml solution containing 1% PBSTM with either a polyclonal anti-Zika E antibody, a polyclonal anti-Zika prM antibody or a polyclonal anti-Zika M antibody at 1:5000, 1:5000, and 1:3000 dilutions respectively (3 separate non-reducing incubations total). Next, membranes containing reduced samples were incubated in a 5 ml solution containing 1% PBSTM with either a polyclonal anti-Zika E antibody, a polyclonal anti-Zika prM antibody or a polyclonal anti-Zika M antibody at 1:5000, 1:5000, and 1:3000 dilutions respectively (3 separate reducing incubations total)**.** The membranes were incubated at RT for 2 hours then washed again in PBST for 5 rounds of 5 minutes each. They were then incubated in a solution containing 1% PBSTM and a 1/5,000 dilution of secondary goat anti-rabbit antibodies at RT for 2 hours. The membranes were again washed with PBST five times for five minutes each, were doused in developing solution (Western Blotting Luminol Reagent 750 µL of Solution A and 750 µL of Solution B, Santa Cruz biotechnology) and were developed.

*2.12 OptiPrep Gradient Preparation*

To visualize the sample, Transmission Electron Microscopy image (TEM) of the VLPs was to be performed, An OptiPrep gradient was set up as shown in Figure 3C. Initially a PEG precipitation took place. In this experiment, a normal large-scale extraction took place except after the supernatant was obtained, 8% polyethylene glycol (PEG) 6000 (Chem Cruz) was added to the supernatant and the supernatant/PEG mixture was spun on ice, after ~2 hrs samples about 20 ml was taken from solution and set aside in -80 °C. The remainder of the sample was allowed to spin on ice overnight-(~10 hrs). The next morning the mixture was spun down at 16,000 g for 20 minutes at 4

°C and the supernatant was separated from the pellet. The pellet was saved and was resuspended in half the original volume of the sample in PBS, creating a 2X protein concentration. The OptiPrep gradients are twice as dense as sucrose gradient but can semi-purify a protein and allow one to view the image under electron microscopy. To separate the plant protein from the Virus-like particles, an OptiPrep gradient which contained 2 ml of 60% OptiPrep gradient at the bottom of the tube, 2 ml of 40% OptiPrep gradient above that layer, 10 ml of 10% OptiPrep gradient above that layer and finally 4 ml of the samples taken after 2 hrs was placed on top (as seen in Figure 3C). Another tube contained the same setup except that instead, the 2x concentrated PEG precipitation were put at the top of the OptiPrep. The gradients were run at 28,000 rpm for 2.5 hours and samples were taken. The interface bands between the 10% and 40% fractions were saved and used for TEM.

*2.13 Transmission Electron Microscopy*

The semi-purified extract of the interface band from the tube that contained the samples taken after 2 hrs was fixed to a TEM mesh and was negatively stained with 1% uranyl acetate. After 5 minutes, the excess stain was removed from the mesh and the mesh was washed twice with ddH2O. The sample was patted with a chem wipe to remove excess water. The mesh was then allowed to dry for 15 minutes before it was imaged with a CM12 transmission electron microscope.

3. Results

*3.1 Plasmid Construction and Colony Screening*

The PCR from the pUC57-ZCME-F vector of the Zika prME gene block yielded the expected size when ran on a 1% agarose gel (~2.2 kb). The PCR from the pBYR2eK2M-BAZE vector of the BASP gene block also yielded the expected size when ran on 1% agarose gel (~240 bp). After restriction digestion, all segments again yielded

the expected sizes on 1% agarose gels: Zika prME: ~2 kb, BASP: ~150 bp, Gemini Backbone: ~12 kb. After purification of these segments was performed and ligation occurred, cells were electroporated and plated. As previously stated, colonies were taken from this plate for a colony screen. All 10 colony screens of cells electroporated with the results of the ligation precipitation displayed growth on kanamycin plates. When subjected to PCR screening with primers 35S-F and SM-Spe-R the correct size was observed for all 10 samples (~700bp). Plasmid preparations were completed for the first 2 samples ran on the gel. When submitted for sequencing the plasmid was found to be correct with no mutations. Agrobacterium strain EHA105 was transformed with the plasmid and a culture was grown over night. Figure 4 below displays the vector in addition to the insert containing the code for the proteins of interest that are displayed in Figure 5.

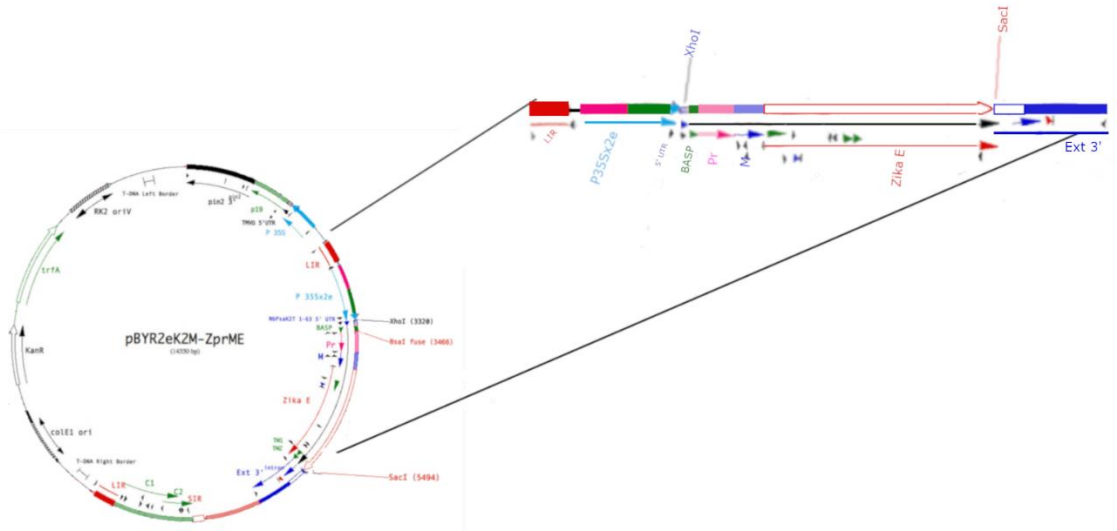


**Figure 4: Final pBYR2eK2M-ZprME Expression Vector: This vector depiction is displaying the detailed insert that codes for protein of interest (as previously described in Introduction section 1.8).**

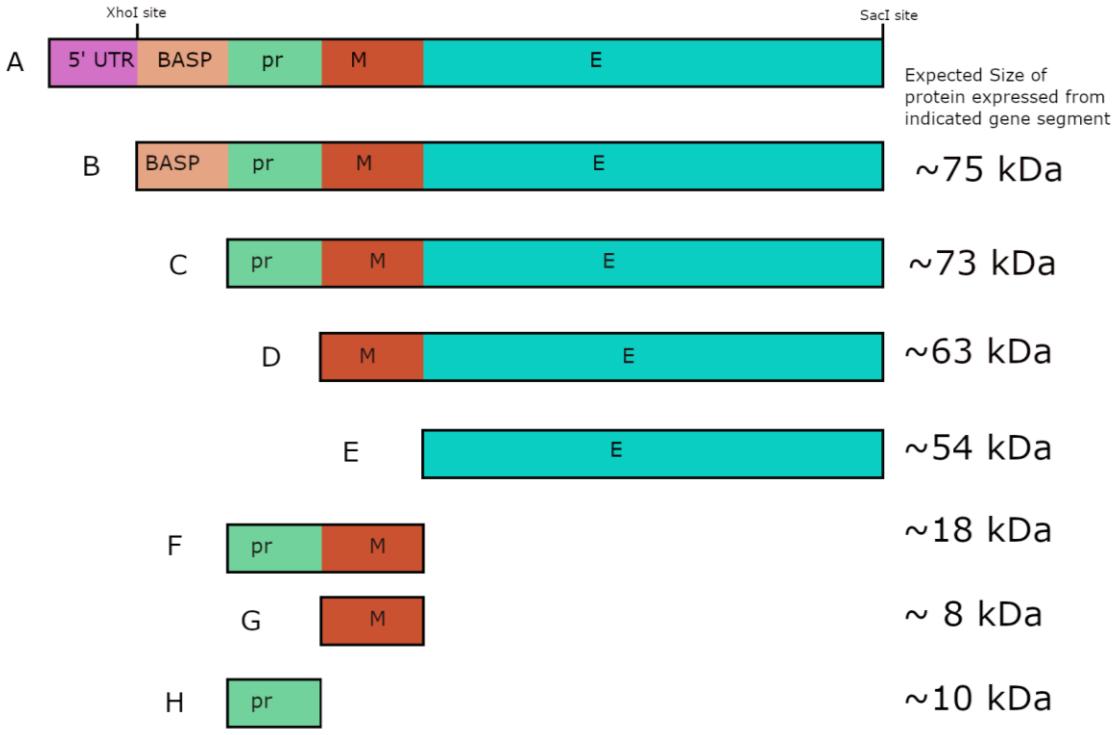


**Figure 5: pBYR2eK2M-ZprME Expression Cassette and Sizes of Functional Proteins that Can be Produced.**

*3.2. Verification of Conformational Zika E Protein Expression in N. benthamiana by Western Blot Analysis.*

To determine if there was expression of the Zika E protein post-infiltration, leaf tissue from construct-infiltrated *N. benthamiana* plants was harvested 4 DPI. In addition, samples from un-infiltrated plants (UN) were also harvested at 4 DPI. Proteins in crude extracts from harvested leaves were resolved by SDS-PAGE and subjected to immunoblotting (Fig. 6A). When probed with a monoclonal antibody (mAb) against the ZIKV E protein domain II-III fusion loop, a major protein band of ~54 kDa was demonstrated (Fig. 6A) in all samples from infiltrated leaves, whether they were extracted with or without Triton X-100 (1%). In contrast, UN leaf tissue samples extracted in either condition did not contain a protein that reacted with the anti-E-

fusion-loop mAb. It is therefore likely that the E protein (expected MW of 54) accumulates in leaves following transient expression with our construct (Fig. 6A).

It was determined whether the produced 54 kDa protein was acid stable, in an effort to optimize future purification conditions. Additional leaf material from the same infiltrated plants was extracted and purified using the acid preparation purification procedure described in the methods section 2.5. In acid prepared UN leaf tissue extracted in PBS or PBS that contained Triton X-100 (1%), there was no signal detected by western blot analysis. Acid prepared infiltrated samples extracted in PBS and a mixture containing both PBS and Triton X-100 detergent both showed signal when probed with the anti-Zika E monoclonal antibody. Both samples showed a signal around ~54 kDa, the expected size of the fully formed Zika E protein (Fig 6B).

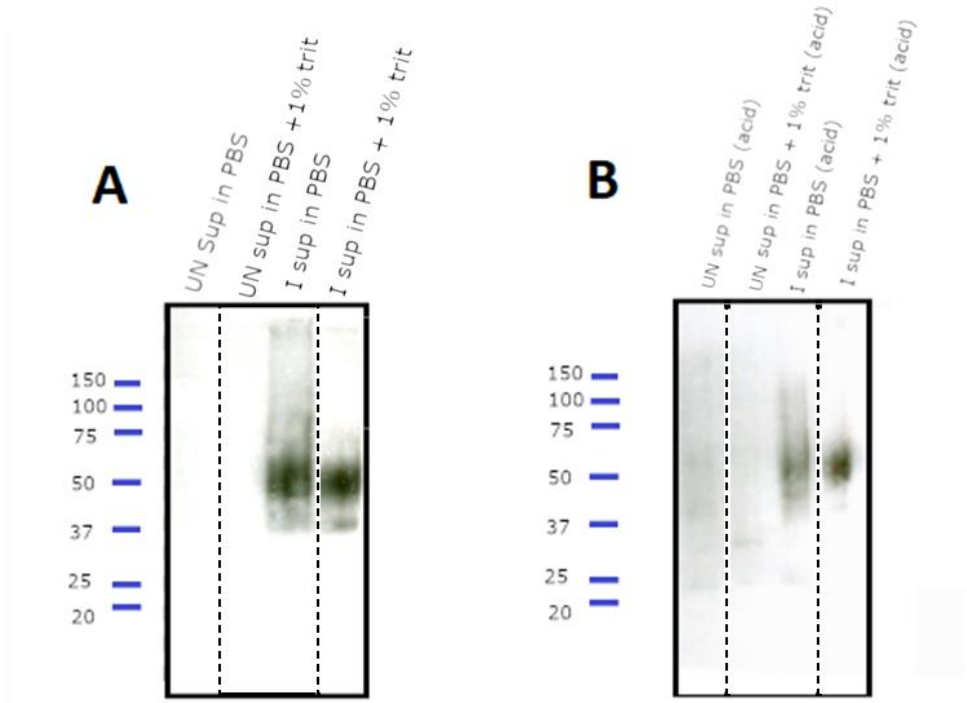


**Figure 6: Verification of Zika E Protein Expression in *N. benthamiana* by Western Blot Analysis. (A) Western blot of Uninfiltrated supernatant (UN sup) extracted in PBS, UN sup extracted in PBS and 1% triton, supernatant from samples infiltrated with construct-infected *A. tumefaciens* (I sup) extracted in PBS, and I sup extracted in PBS and 1% triton. All samples were probed with an anti-Zika E monoclonal that targeted the Zika E protein domain II-III fusion loop. (B) Western blot of uninfiltrated supernatant (UN sup) extracted in PBS and purified by acid preparation (acid), UN sup extracted in PBS and 1% triton (acid), supernatant from samples infiltrated with construct-infected *A. tumefaciens* (I sup) extracted in PBS (acid), and I sup extracted in PBS and 1% triton (acid). All samples were probed with an anti-Zika E monoclonal that targeted the Zika E domain II-III fusion loop.**

*3.3 Time Course to Determine peak Zika E Protein Expression*

A time course was completed to determine which day was optimal for taking leaf tissue in future studies, based on the degree of ZIKV E protein present. Construct infected leaf material that was run under non-reducing conditions consistently yielded recognizable bands around the 54 kDa range, the size of the ZIKV E protein, while samples under reduced conditions did not reveal prominent bands in the ~54kDa range when the same samples were probed with both the conformational monoclonal anti-Zika E antibody (Fig. 7A) and when probed with the polyclonal anti-Zika E antibody (non-

conformational) (Fig. 7B). Under non-reducing conditions the conformational antibody displayed the most intense bands at 3 and 4 DPI. With the lowest intensity at 5 DPI. Upon quantitative analysis, it was determined that 3 and 4 DPI contained similar intensity of bands (Fig. 7C). When samples were under reducing conditions and probed with the same monoclonal antibody previously described, the most intensity was seen at 2 DPI and the intensity of the bands decreased each sequential day (Fig. 7A and 7C).

Far more degradation product was detected by the polyclonal antibody probe than in the monoclonal antibody probe. However, the intensity of these bands was not tested since the main interest is in the presence of the fully formed Zika E protein. The intensity under nonreducing conditions was found highest in Day 5 samples when probed with anti-Zika E polyclonal antibodies (Fig. 7B and 7C). When these samples were run under reducing conditions and probed with the polyclonal anti-Zika E antibody, signal was not detectable on the western blot (Fig. 7B) and the intensities were almost non-existent (Fig. 7C) and could be attributed to background.

It should be noted that these interpretations are not exact and although they are quantitative, only provide rough estimates.

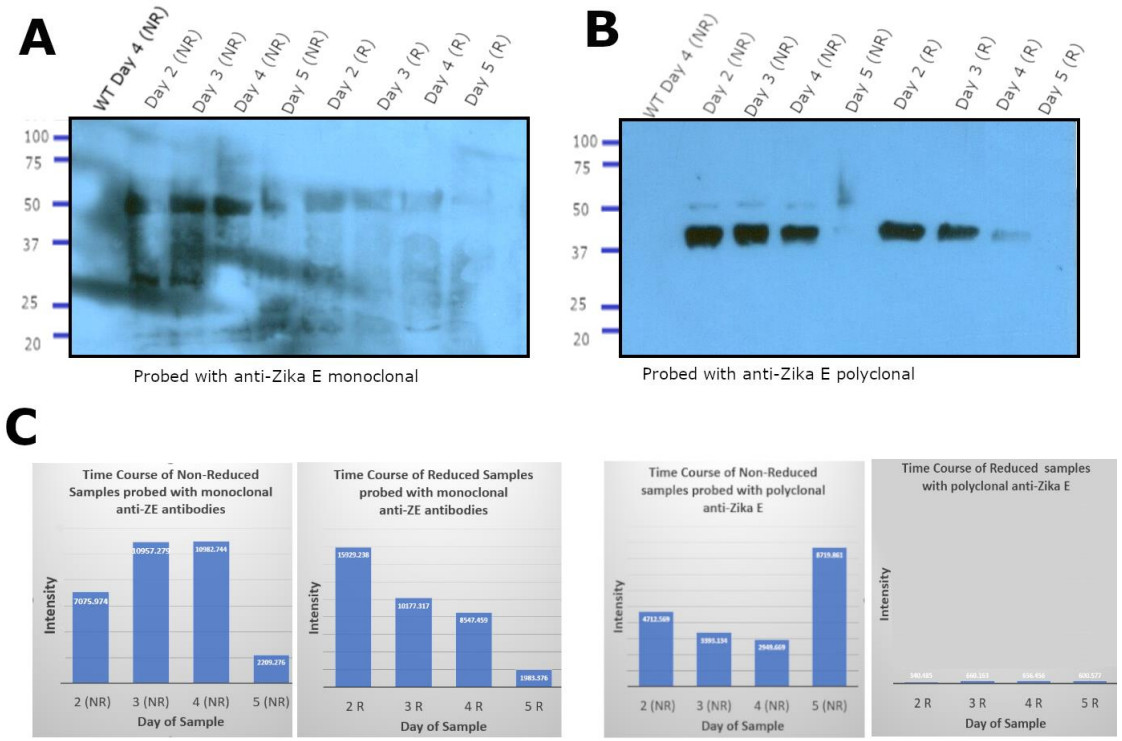


**Figure 7: Time Course to Determine Day of Highest ZIKV E Protein Expression: (A) Western blot of leaf tissue samples picked on 2, 3, 4, 5 DPI ran under both reducing and non-reducing conditions and probed with conformational monoclonal anti-Zika E. (B) Western blot of leaf tissue samples picked on 2, 3, 4, 5 DPI ran under both reducing and non-reducing conditions and probed with polyclonal anti-Zika E. (C) Kinetic analysis of the westerns in (A) and (B) to quantitatively determine the approximate intensity of each band.**

*3.4 Determination of Protein Solubility*

It was imperative to determine if all the previously detected Zika E protein was in the soluble fraction or insoluble fraction of the homogenate. At this point in the study antibodies were also acquired that detected Zika prM and M proteins. To this end, we have used differential centrifugation following various treatments as outlined in Figure 3. The supernatant samples from all stages of the experiment and the resuspended final pellet were resolved by SDS-PAGE and subjected to immunoblotting using the anti-E-fusion-loop mAb as a probe (Fig. 8A). Importantly, all the E protein that accumulates in plants that also can react with the mAb can be found in the aqueous fraction (first supernatant, Fig. 8A lane 1). Additional reactive E-protein cannot be extracted from the water-insoluble pellet by increasing concentrations of the neutral detergent Triton X-100 (Fig. 8A, lanes 2-4) nor can we detect additional reactive E protein in the remaining pellet (Fig. 8A lane 5). Since the anti-E-fusion-loop mAb cannot detect the E protein if it is denatured, the samples were never run under reducing conditions then probed with this antibody.

When samples were probed under non-reducing conditions and probed with polyclonal anti-Zika prM, there was signal detected in the soluble fraction that was removed directly after centrifugation mainly slightly above 37 kDa and slightly around 50 kDa. There was also slight detection in the soluble fraction obtained after centrifugation of the pellet in 1% Triton X-100 + PBS (Fig. 8B). There was no signal detected in the pellet for this trial. In addition, all samples that were ran under reducing conditions did not display significant signal (Fig. 8B).

When the samples were probed with a polyclonal anti-Zika E antibody under non-reducing conditions, there was again signal detected in the soluble fraction that was removed directly after centrifugation. This signal was slightly above 37 kDa and slightly

below 50 kDa. There was also slight detection in the soluble fraction obtained after centrifugation of the pellet that was resuspended in 0.1% Triton X-100 + PBS and 1% Triton X-100 + PBS, this signal was also slightly above 37 kDa and slightly below 50 kDa. The pellet under non-reducing conditions did not display any signal (Fig. 8C). When ran under reducing conditions and probed with the polyclonal anti-Zika E antibody, the only significant signal was seen in the pellet. This band was also higher than the other bands detected on the same gel at slightly above 50 kDa (Fig. 8C).

When these same samples were running under both reducing and non-reducing conditions and probed with a polyclonal anti-Zika M antibody, there was signal in almost every lane at a band estimated to be around 30 kDa. It was determined later in the study that these bands were a reaction to plant protein as supported in Figure 10D. Excluding the bands that displayed signal because of cross-reactivity to plant protein, the only significant band that displayed signal was seen in the soluble fraction of the pellet that was resuspended in PBS + 1% Triton (Fig. 8D). This band was slightly above the 50 kDa.

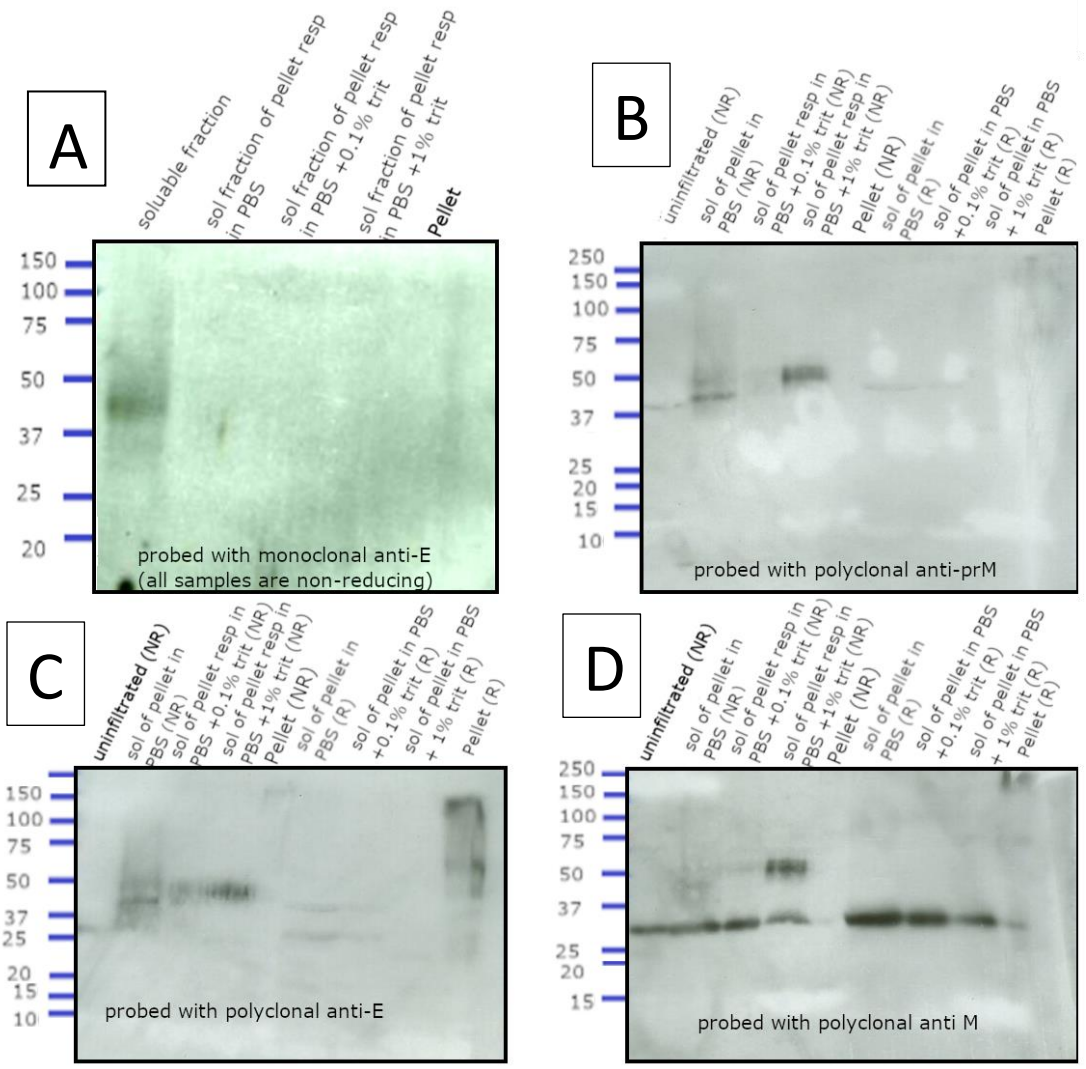


**Figure 8: Western Blots with Samples that Each Were Extracted by Increasingly Stressful Means (A) Samples probed with monoclonal anti-Zika E antibody ran under non-reducing conditions only. (B) Samples probed with polyclonal anti-prM under both reducing and non-reducing conditions. (C) Samples probed with polyclonal anti-E under both reducing and non-reducing conditions (D) Samples probed with polyclonal anti-Zika M under both reducing and non-reducing conditions.**

*3.5 Western Blot Analysis of Sucrose Gradient to Determine VLP Formation.*

There have not previously been studies where Zika VLPs express the Zika pr, M or E proteins in plants. Under these circumstances, methods detailing isolation of the

supposedly formed particle have also not previously been completed. To isolate the particle a series of sucrose gradients were performed. Primarily, supernatant from infiltrated plant extract was run on a sucrose gradient that contained 10%, 20%, 30%, 40% and 50% sucrose. When probed with a Zika anti-E conformational monoclonal antibody, which targeted the Zika E protein domain II-III fusion loop, signal at ~54 kDa was seen in all samples except for the 40% fraction. In addition, there was a band seen slightly above 150 kDa that was also detected in all gradient samples tested. Signals were strongest in the supernatant and the 10% fraction, in which both a ~54 kDa and a ~38 kDa degradation product were detected (Yang *et al.*, 2018). However, the ~38 kDa degradation product began to disappear as the gradients became denser in the 20%, 30% and 40% fractions (Fig. 9).

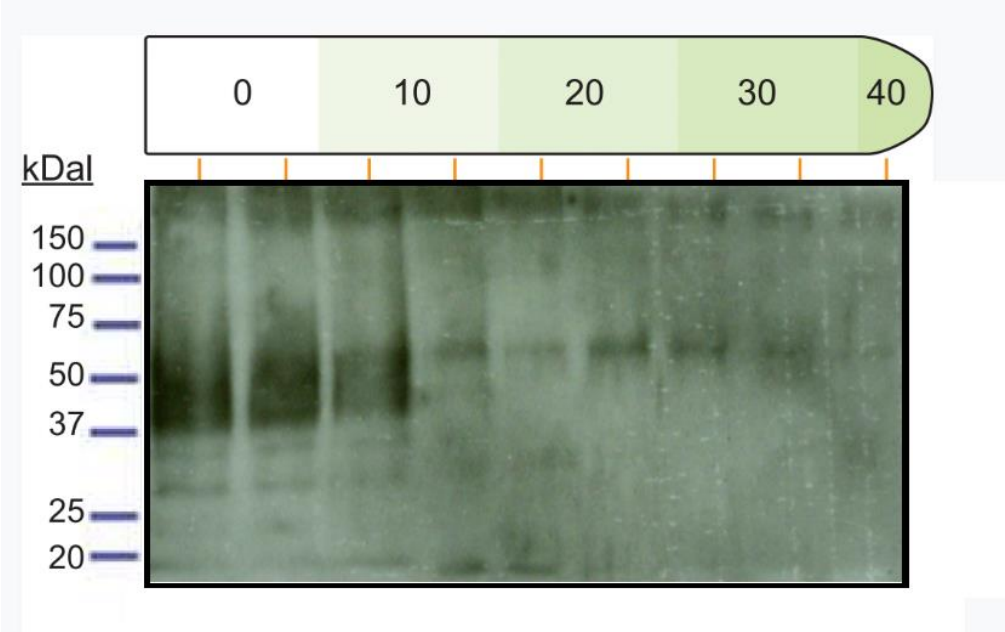


**Figure 9: Western Blot Analysis of a Sucrose Gradient to Determine Rate at Which Identified Recombinant Zika E Protein Travels. The supernatant (sup), 10% fraction (10%), 20% fraction (20%), 30% fraction (30%), 40% fraction (40%) and 50% fraction (50%) were ran on the gel above after running the sucrose gradient cycling at 28,000 rpm for 2.5 hours.**

*3.6 Western Blot Analysis of Concentrated Sucrose Gradient Samples Using Different Ab Probes.*

Extractions from construct infiltrated leaf tissue were ran on a 20%:70% sucrose gradient to create a concentrated interface band, as previously described in the methods section and seen in Figure 3B. When a sample of the interface band was taken from the same extraction and sucrose gradient run and probed with different polyclonal antibodies, a signal was seen in all probes at ~75 kDa (Fig 10. A-C), the expected size of the full uncleaved Zika prME expression cassette. When probed with a polyclonal antibody targeting the Zika E protein, there was a signal detected at ~54 kDa, the expected size of the fully formed Zika E protein (Fig. 4, Fig. 10 A Lane 6). There was no signal detected at ~54 kDa when the samples were probed with polyclonal antibodies that targeted the Zika prM protein or polyclonal antibodies that targeted the Zika M protein (Fig. 10 B and C).

Finally, there was no signal below the 15 kDa marker when the interface sample was probed with the polyclonal anti-Zika E. However; there was a signal band detected below the 15 kDa marker in both samples probed with either the polyclonal anti-Zika prM or the polyclonal anti-Zika M. The expected size of Zika prM and Zika M proteins when expressed are ~10 kDa and ~8.5 kDa respectively. When probed with anti-prM, there were multiple segments detected in the 0% sucrose, 20% sucrose and interface sections of the gradient that were below 15 kDa. In addition, it was also noted that there was a small band present just above the 25 kDa range in a lane of sucrose gradient samples in the 20% fraction, that were probed with anti-prM.

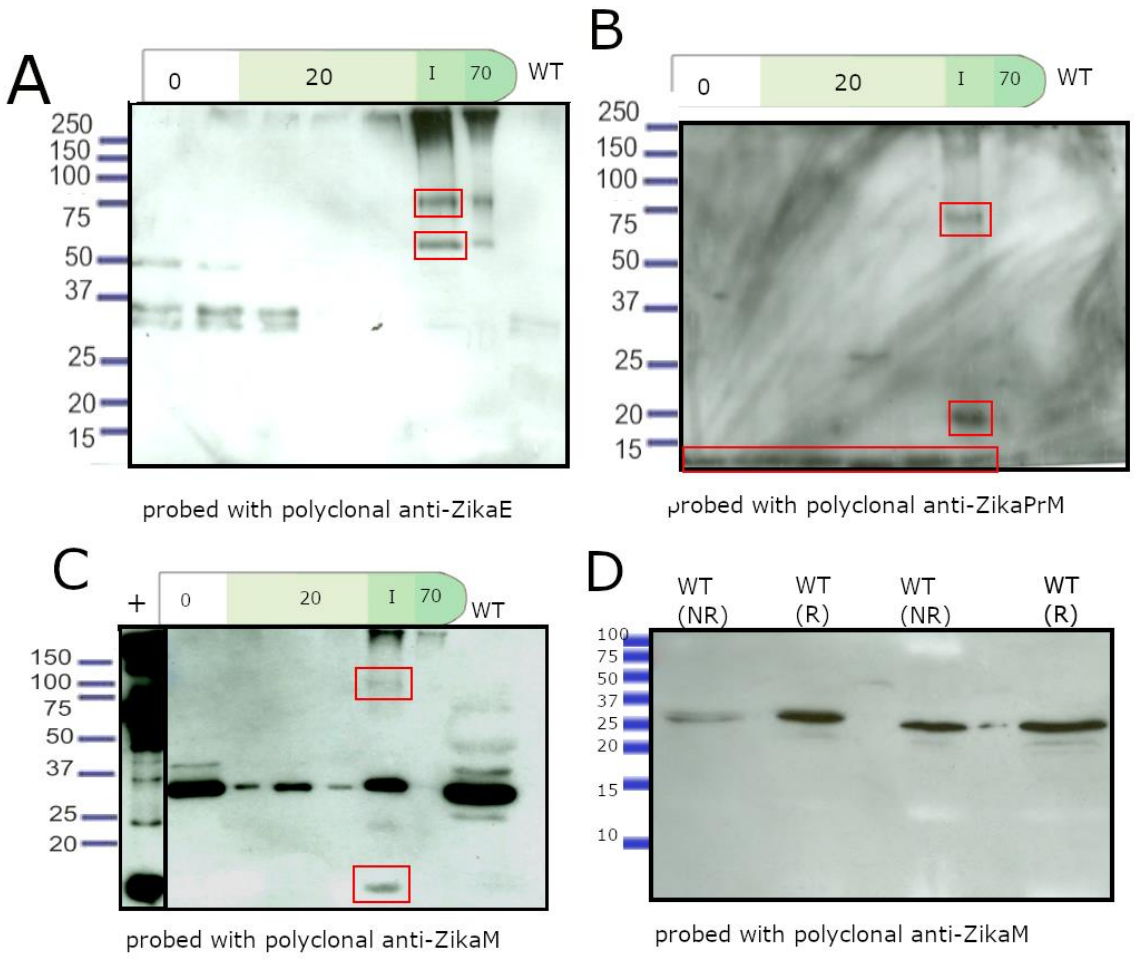


**Figure 10: Western Blot Analysis Comparisons of Construct Infiltrated Supernatants Ran on a 20%,70% Sucrose Gradient. (A) Western blot probed with a polyclonal antibody targeting the Zika E protein (poly anti-Zika E). (B) Western blot probed with a polyclonal antibody targeting the Zika prM protein (poly anti-Zika prM). (C) Western blot probed with a polyclonal antibody targeting the Zika M protein (poly anti-Zika M). (D) Supernatant of UN plant probed with anti-M antibody to determine non-specific binding of antibody.**

*3.7 Transmission Electron Microscopy of Expressed Proteins*

TEM revealed particles present just beneath a 10% optiprep gradient and above a 60% optiprep gradient after sampling using methods previously described. Micrographs revealed a particle that was ~100-120 nm wide (Fig. 11). The size of the plant-produced

VLPs is the similar to the expected size of ZIKV particles that bleb from the endoplasmic reticulum (Salvo *et al.*, 2018).

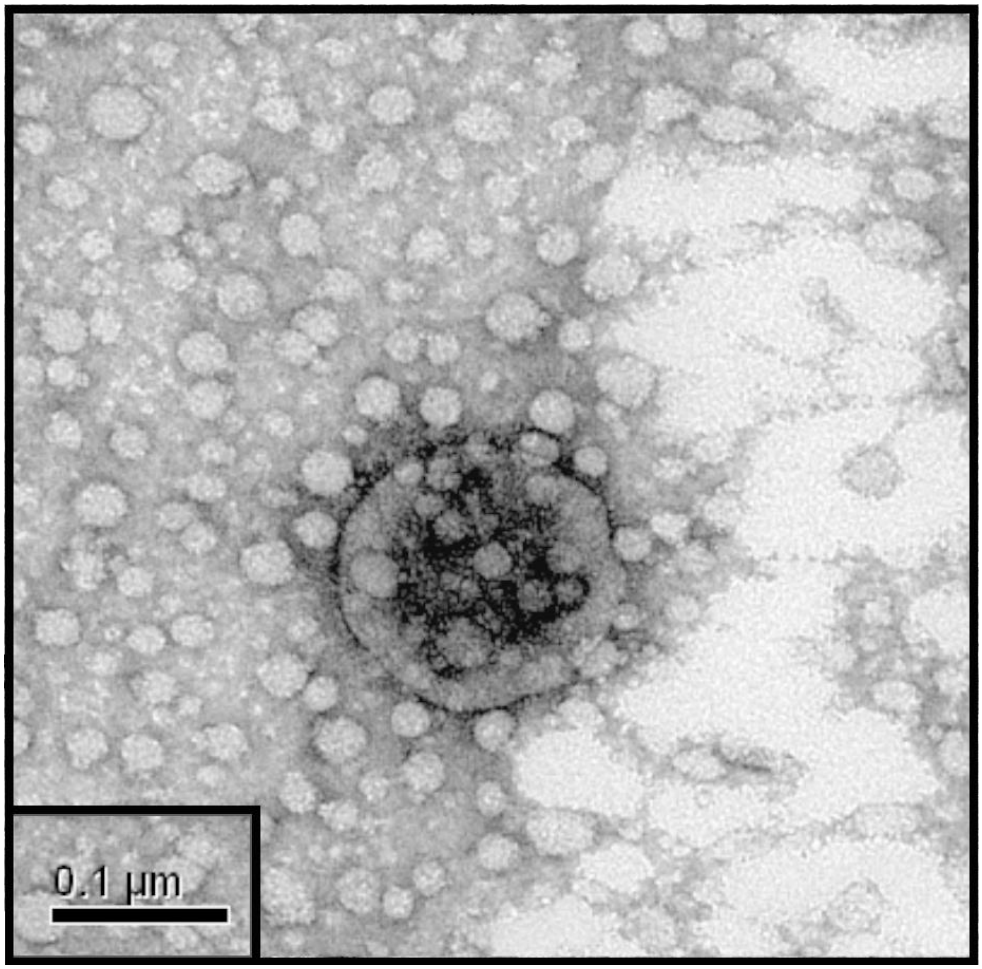


**Figure 11: Transmission Electron Micrograph of Semi-Purified Plant-Expressed Particle.**

# 4. DISCUSSION

The systems utilized in this study have the potential to achieve the requirements needed for an expression system to combat against future infection with ZIKV. The vector used in this study, BeYDV, has long been shown to produce protein in high yield and in a short amount of time (Mor *et al.*, 2003). In addition the agroinfiltration techniques used in this study could be translated to the larger scale production of the VLP in this study, needed to create a ZIKV vaccine, through processes like vacuum infiltration (Matsuo *et al.*, 2016). Presence of proper ZIKV epitopes was also demonstrated in this study in addition to overall cost effectiveness of the methodology.

The aim of the expression cassette was initially to produce the BASP protein in addition to the pr, M, and E proteins of ZIKV. If uncleaved, there would appear a 75 kDa band and if cleaved the E protein should appear around 54 kDa, the M protein should appear around 8 kDa and the pr protein should appear around 10 kDa (as depicted in Figure 5). In theory, these proteins would self-assemble as VLPs by blebbing out of the plant ER membrane and these VLPs would contain conformational epitopes like those of the native Zika virus. The DNA sequence that encoded the prM was included in an effort to produce a conformationally correct Zika E protein, as the Zika prM is believed to aid in the correct conformational scaffolding and folding of the E protein during viral maturation (Lorenz *et al.*, 2002). The Zika E protein is arguably the most important of the proteins contained in the production of the VLP, as it is the target for the largest amount of neutralizing antibodies by host infected cells (Dai *et al.*, 2016). For this reason, correct folding of the Zika E protein is sought after.

Initial findings in this study tested the mere presence of any of the proteins encoded by pBYR2eK2M-ZprME expression cassette in the soluble fraction of the extraction. The presence of the Zika E protein in the soluble fraction at the expected size

of the E protein (~54 kDa) indicates the protein is being secreted in virions by the plant infected cells. The sub viral particles assemble in the ER of the cell. It is then transported through the TGN, at which point the immature particle is cleaved by furin (in humans) and is exocytosed from the cell (Mukhopadhyay *et al.*, 2005). A protein in the leaves of tomato plants has been identified as a furin-like protease that cleaves a protein known as systemin into smaller polypeptides and likely contributes to the processing of prME in plants within this study (Schaller and Ryan, 1996). Prior to this cleavage event of the immature particle by furin, the particle undergoes multiple cleavage events in the ER by host signal peptidases (Y. Zhang *et al.*, 2003).

In this study the VLPs likely blebbed from the ER membrane, similar to the native virus (Hasan *et al.*, 2018). Such an occurrence would cause the particles to be in the soluble fraction. This result is seen in Figure 6A, in both the leaf tissue sample extracted in PBS and in the sample extracted in PBS and 1% Triton. Both samples also appeared to display bands of the same intensity when the soluble fraction was tested. This result also indicates the addition of the Triton X detergent did not cause a major difference in the amount of conformationally correct Zika E proteins extracted from the sample that could be detected by the monoclonal antibody that targeted the Zika E domain II-III fusion loop. It should be considered that this antibody is more likely to target proteins that are transitioning from their immature state to their mature state, since the Zika E domain II-III fusion loop (residues 98-109) is normally buried by domains I and II of the other ZIKV E monomer. The fusion loop is generally only displayed between virus entry between a host cell and viral membranes (Dai *et al.*, 2016). Though the antibody could likely still target the epitope, it might be possible that more Zika E is present in the samples that does not display signal when probed with the monoclonal antibody. It is also possible that there is protein containing this epitope that

was never cleaved from the M and pr proteins (~75 kDa) but that the other proteins hinder the display of the fusion loop and as a result hinder the detection of the E protein, even if those proteins are conformationally correct. This result still demonstrates the ability for a conformationally correct Zika E protein to be formed through means of plant expression and provides hope that the protein may be secreted in virions.

The second portion of the experiment displays the acid stability of the formed Zika E protein. During the acid precipitation, isoelectric points of proteins and their repulsive electromagnetic forces are meant to cancel one another out and equal zero. Such an event causes protein aggregation to occur and can result in a much purer final product. Past studies have also shown that acid preparation techniques like the one used in this experiment are able to remove unwanted plant proteins such as Rubisco from the sample (Diamos and Mason, 2018). The samples that were subjected to acid preparation (Fig. 6B) displayed approximately the same intensity, when probed with the Zika E monoclonal antibody, as the samples that did not undergo acid precipitation when they were developed using the same conditions. Such findings indicate that the Zika E protein produced by our methods can be purified using acid preparation techniques without loss of conformation of the protein or loss of significant yield.

The results of the time course allowed for peak expression to be determined. Through the use of ImageJ software, as described in the methods, the approximate intensity of the bands present on the developed membrane were able to be determined. Since the samples from day 3 and 4 DPI were both the highest intensity and almost the same under non-reducing conditions when probed with a monoclonal anti-Zika E antibody, day 4 was used in the experiments (Fig. 7A, C).

Further tests supported the hypothesis that the majority of the conformationally correct Zika E protein was present in the soluble fraction. By following the procedure

represented by the schematic in Figure 2, the insoluble fraction (pellet of the homogenate) was exposed to increasing concentrations of detergent as well as additional irritation by metal beads, which in theory would increase protein released from samples. The hope was if additional correctly folded Zika E proteins were in the insoluble fraction then the increased stress on the leaf tissue would allow them to solubilize which would allow optimal amounts of protein to be obtained in future experiments. Though increasing amounts of detergent were added to the pellet, there was only signal in the supernatant sample when probed with the conformational anti-Zika E monoclonal antibody (Fig. 8A). Such results indicate the protein of interest is likely forming a virion and allowed us to continue running tests on the soluble fraction rather than on both the soluble and insoluble fraction. Since the monoclonal antibody used was seen to only efficiently recognize conformationally correct proteins (Fig. 7A), we were only able to run the first experiment under non-reducing conditions. The same samples were again run under both reducing and non-reducing conditions in an effort to see if more protein epitopes would be exposed to the polyclonal antibodies when the proteins were subjected to high amounts of SDS and heat. When probed with anti-prM the sample that showed the strongest band was just over 50 kDa range in supernatant sample of the pellet that was resuspended in PBS+1% triton (Fig. 8B). Since this antibody probe detected both the pr and M proteins, the ~50 kDa fragment could be many variations of proteins. Though unlikely due to size, it is possible that it is the Zika E with the M protein attached. Though there is expected band size for such a protein is much larger than this, as indicated in Figure 5. This result also indicates that the membrane portions of the protein might have trouble solubilizing, since so much of it was only detected under reducing conditions in the pellet. This would indicate possible different methods of protein extraction in the future.

The gel that used the same samples and was probed with a polyclonal anti-Zika E showed strong bands in the reduced pellet. This is likely because the antibody was produced using a peptide that contained denatured epitopes. As a result, the antibody is more likely to see the protein of interest when it is probed against a denatured sample (Fig. 8C). This band appeared just above the 50 kDa range, this is close to the expected size of the Zika E protein. Finally, the last gel was probed with an anti- Zika M antibody and most prominent band was seen in the non-reduced soluble fraction that came from the pellet extracted in 1% triton. This could indicate that the M proteins denature when exposed to reducing conditions. The bands seen in every row between the 25-37 kDa range are likely plant proteins, this will be further explained in Figure 10D.

The sucrose gradient tests were initially meant to determine protein density. The sucrose gradient setup displayed in (Fig. 3A) was meant to provide sucrose gradients of variable density that would allow us to determine approximately which gradient the particles no longer are able to travel though. As seen in (Fig. 9), The first few lanes contain the supernatant and the 10% fractions. The degradation product of the Zika E protein is seen in both of these samples at ~ 38 kDa (Yang *et al.*, 2018). It is thought that this formation of the protein is not fully formed and as a result might not elicit the same degree of protective immunity against ZIKV infection.

In a sucrose gradient, particles travel until they reach the point where their density matches the density of the surrounding sucrose (Noll and Noll, 1989). The rate at which they travel can be different for each VLP. As seen in Figure 9, the bottom half of the 20% fraction has the highest intensity band around ~54 kDa and the top layer of the 30% fractions continues to display the same band. The bottom layer of the 30% fraction and the top layer of the 40% fraction display progressively less intense bands at ~54 kDa. This could be due to error in fraction separation when removing the sucrose samples

from the initial sucrose gradient tube or could also be aggregated material of the same ~54 kDa proteins that are present in the 20% fraction that began to separate when they reached a denser fraction. It is important to note that the ~38 kDa fragment that is present in the soluble fraction and the 10% fraction completely disappears in the deeper fractions, indicating that it does not encompass the density of a VLP and is likely not a fully formed version of the protein of interest. In each row there also appears to be a band at the very top of the gel at ~150 kDa. This band is likely aggregation of the Zika proteins that formed. It is also twice the size of the expression of the prME proteins in unison (~75kDa). Further tests were performed to determine if other protein components were also present in the sample and if VLPs were formed.

The presence of the Zika pr and M proteins in the samples could affect the efficacy of the resulting VLP upon immunization trials (Lorenz *et al.*, 2002). Primarily, sucrose gradients were run following the schematic in Figure 3B, to concentrate whatever VLPs were present in the sample. The prior experiment determined the VLPs generally pass through the 20% sucrose fraction and into the 30% sucrose fraction, but largely are not present in the 40% fraction. It would be likely all Zika virus-like particles in future experiments within this study would pass through a 20% sucrose fraction but would not be able to pass through a 70% sucrose fraction and would form an "interface" band, that would contain the majority of proteins present in that sample. Having a concentrated sample would allow for easier detection of proteins when analyzed by western blot as they would be more likely to appear upon probing with an antibody. Samples were observed under both reducing and non-reducing conditions. When samples were observed under non-reducing conditions, only very light signal was seen in the 54 kDa range when probed with a polyclonal anti-Zika E, absolutely no signal was seen in the regions of interest when probed with the polyclonal anti- Zika prM antibodies

and the polyclonal anti-Zika M antibodies. It is likely that all epitopes which the antibodies were raised to react against were hidden when the proteins were ran under non-reducing conditions and these epitopes could eventually display and be detected for signal by HRP linked antibodies when ran under reducing conditions.

When probed with a polyclonal anti-Zika E antibody, under reducing conditions, bands were visualized at ~75 kDa and ~54 kDa, the expected sizes of the full Zika BASP, pr, M and E proteins seen in (Fig. 4) A and expected size of the full Zika E protein, respectively (Fig 4 E). When probed with the polyclonal anti-Zika E, there was no signal detected below or around the 15 kDa range. When probed with polyclonal anti-Zika prM antibodies, there was a signal detected again in the ~75 kDa range and below the 20 kDa range in the "interface" sample. For this sample there was no signal detected in the 54 kDa range. Such results indicate the previously viewed ~75 kDa fragment contained both the Zika E protein and wither the Zika pr, the Zika M or both. There was no 54 kDa fragment in this sample further supporting that the 54 kDa band seen in the previous sample was the Zika E protein (Fig. 10A, B). The band below the 20 kDa range could have been either the Zika pr (~10kDa), the Zika M protein (~8 kDa) or aggregation of both. It is important to note that there were also bands present in the 0%, 20% sucrose samples as well as the interface sample that were below 15 kDa. These bands were not present in the 70% sucrose or in the wildtype. They were also not present in the gels that were probed with anti-Zika E or anti-Zika M. These bands could have been cleaved pr. There was additionally a band seen below the 25 kDa but above the 20 kDa range in the 20% fraction of material (Fig. 10B). It is thought that this signal could also be indicative of pr, which should occur in the situation of mature VLP formation, that likely aggregated and would not be dense enough to travel to the "interface" (Lorenz *et al.*, 2002; Y. Zhang *et al.*, 2003).

To determine whether the segment below 20 kDa was the pr or the M, the same "interface" sample was probed with polyclonal anti- Zika M antibodies. It was determined that the ~75 kDa fragment was still present and that the fragment below the 20 kDa range also continued to display signal (Fig. 10C). Such results indicate the presence of the Zika M protein in the ~75 kDa fragment and that the band just below 20 kDa that appeared in gels probed with both anti-Zika prM and anti-Zika M was likely the Zika M protein. It is likely then that the segments found beneath the 15 kDa range were the Zika pr protein since they did not appear when probed with anti-Zika M. Based on the size and the signal of the proteins present, it was determined that expression of the Zika pr, M, and E proteins were achieved.

In addition, ZIKV has 6 sites of glycosylation in its envelope and 4 sites of glycosylation in its membrane (Gupta *et al.*, 2016). Such a circumstance could cause the estimated 63kDa protein (Fig. 4) to appear larger on a gel, indicating that that the ~75 kDa fragment viewed on the developments could be the fully formed, glycosylated Zika ME protein with pr cleaved off.

We were never able to run samples that were probed with the Zika E monoclonal antibody as reducing samples because the monoclonal was conformational and would not recognize any of the proteins in their denatured states. The experiment displayed in Figure 10 was also run under non-reducing conditions (results not show). In these tests, he proteins were not able to be visualized at the 75 kDa range. This likely is because epitopes were hidden and even if they were present, were not able to be visualized by western blot as a result. Considering this find, it is possible there were ~75 kDa fragments or ~63 kDa fragments in those samples but that they were never able to be visualized due to the nature in which the antibodies recognized epitopes.

The next step in the process of determining VLP formation was visualization of the proteins and determination of the size. To do this a semi-purified preparation of the material was to be made. To increase the yield of protein and VLP formation, PEG was added to the isolated supernatant. PEG precipitation has been shown to aid in the accumulation of protein and when used above a concentration of 6% has been shown to aid in the formation of VLPs that mimic other viruses (Diamos and Mason, 2018b). OptiPep, unlike sucrose, can be viewed under a TEM microscope without the need for dialysis (Van Veldhoven *et al.*, 1996). Optiprep was used for this reason to isolate the VLP and visualize the components of certain fractions. The Optiprep gradient was set up as is shown in Figure 3C. OptiPrep gradients are also twice as dense as sucrose gradients. For this reason, it was predicted that the VLPs would travel through the 10% OptiPrep gradient and would remain above the 40% gradient. When the sucrose gradients were performed, plant proteins were seen in the 70% sucrose as well as the bottom of the tube. For this reason, it was determined the plant proteins could be isolated as well, as they would pass into but not past the 40% Optiprep gradient and be separated from the VLPs. TEM was thus performed on the "interface" band present between the 10% and 40% fraction of the OptiPrep gradient after centrifugation.

When TEM was performed on the interface band tested under TEM was taken from the gradient that contained the 2 hr PEG precipitation since the overnight PEG precipitation was much greener in color and oversaturation of proteins viewed under the TEM was trying to be avoided. The TEM taken from the OptiPrep gradient particles that resembled those of Zika virus were visualized at about 100 nm-120 nm (Fig. 11). This size correlates with the expected size of formed VLPs that assemble in the ER, as viral particles can be a range of sizes depending on their method of formation (Santi *et al.*, 2006).

This research demonstrates the ability for plants to produce native ZIKV proteins. These findings could aid in the creation of a ZIKV vaccine candidate of low cost, high scalability and efficient immunogenicity. The low cost of plant production can have a huge impact on the ability to distribute and administer vaccines. Plants are able to produce extensive amounts of biomass and resultant protein using far less capital than requirements to produce the same product in cell-culture facilities (Chen and Davis, 2016). This study also demonstrates that the utilization of a geminiviral vector is able to produce recombinant protein that at a rate faster than other vectors utilized in plant biotechnology past studies (Yang *et al.*, 2018).

The BeYDV system containing the Zika prME expression cassette (Fig. 5), was able to produce protein very quickly through agroinfiltration in this study, as shown in Figure 7. It is imperative to note that protein was produced in a conformationally correct way as early as 2 DPI (Fig. 7A, C) using this system. Such circumstances indicate that the system could be used to produce protein even quicker than 4 days if circumstances require the therapeutic immediately. In addition, the BeYDV used in this study was able to produce peak protein expression of Zika E in only 4 days, as compared to previous studies that utilized ICON expression systems and were able to produce Zika E protein at peak levels at 6 DPI (Yang *et al.*, 2018). Degradation products below 54 kDa were detected in this study as well as previous studies that aimed to produce the Zika E protein (Yang *et al.*, 2018). Elimination of this segment can be performed through density gradients that separate the proteins and dialysis or other purification methods to isolate only the correct 54 kDa fragment.

Expressing the Zika E and M proteins contain complications. One such complication is the fact that both the E and M protein require proteolytic processing. As shown in Figure 1, processing of these proteins requires both signal peptidases and Golgi

proteases. Both proteases originate in the host system ER and TGN. Not all prM-E heterodimers are cleaved by furin though and uncleaved heterodimers will revert back to immature trimeric structures (Dai *et al.*, 2016). Since enzymes in plants are different, the proteins produced in plants might not be cleaved as easily as when they are produced in humans. Though studies on plants have determined the presence of furin-like proteases (Schaller and Ryan, 1996) in some plants, it is not yet known if plants contain the same ER signal peptidases that are needed for proper cleavage of the Zika polyprotein (Fig. 1). Other studies have successfully produced flavivirus membrane proteins in various expression systems other than plants such as DENV membrane proteins in mammalian cells (Bray and LAl, 1991), Japanese Encephalitis virus (JEV) membrane proteins through DNA vaccines (Konishi *et al.*, 1998) and production of JEV membrane proteins in HeLa cells and in modified mammalian cell lines (Konishi *et al.*, 2001, 1992). Each of these trials successfully produced flavivirus membrane proteins and most were able to test for and elicit an immune response upon viral challenge (Bray and LAl, 1991; Konishi *et al.*, 1998, 1992).

Signal peptidases are enzymes that cleave the signal peptides from the end terminals of some secretory and membrane proteins in an effort to produce the mature forms of these proteins. They are ER-derived serine proteases that originally isolated in mouse myeloma cells (MILSTEIN *et al.*, 1972). Orthologs of both signal peptidases and signal peptidase-like proteins have been identified in vertebrates, plants and eukaryotes as highly conserved sequences within each (Voss *et al.*, 2013). These peptidases as needed to cleave and process prME (Fig. 1) and their high conservation makes it likely that such events will occur when proteins containing signal peptidase cleavage sites are produced in plants (Ponting *et al.*, 2002; Voss *et al.*, 2013).

Correct processing of the Zika prME also requires cleavage by a Golgi protease known as furin (in humans). The proposal that pr is cleaved in this study is supported by the existence of furin analogs in plants (Schaller and Ryan, 1996). A furin-like protease has been identified in the leaves of tomato plants and potato plants. This enzyme cleaves a protein known as systemin into smaller polypeptides and likely contributes to the processing of prME in plants within this study (Schaller and Ryan, 1996). The protein was termed SBP-50 and it was thought to have held similarity to members of kez2p-like proteases. These kez2p- like proteases allow for maturation of peptide hormones (Schaller and Ryan, 1996). The presence of both these signal peptidases and furin-like proteases support the ability for plants to correctly process the Zika prME and supports the cogency of the results found in this study.

For a particle to be considered a VLP, it must contain dense, repetitive arrays of one or more protein subunits that have high advantage of use in eliciting an immune response (Chackerian, 2007). The dense repetitive arrays allow for crosslinking of a BCR after an antigen is presented to it, such a circumstance allows for B cell activation and eventual formation of a long lived adaptive immune response (Bachmann and Zinkernagel, 1997; Zabel *et al.*, 2013). In order for this dense repetitive array to exist within the viral particle, not every portion of the native structural viral polyprotein must be present. Though Zika Virus is comprised of three structural proteins the (C, E, M proteins) (Davidson, 2009; Hasan *et al.*, 2018), not all proteins are required to create the repetitive arrays needed in a VLP to elicit an adaptive immune response within a host. For this reason, it is not believed that the ZIKV C protein is needed in VLP formation or that its inclusion would produce drastically different results in terms of elicitation of an immune response. The C protein of ZIKV aids in packaging the viral genome and formation of the nucleocapsid core (Hasan *et al.*, 2018), while the E protein elicits the

largest amount of neutralizing antibodies when present in a host and the pr (initially presented as the prM) allows for proper folding of the Zika E protein (Dai *et al.*, 2016; Hasan *et al.*, 2018). The C protein is not necessary for immune responses as it does not carry a large role in eliciting immunogenicity and therefore does not need to be included in the VLP.

Past studies that have excluded the C protein in DENV VLPs found similar efficacies, in terms of immune response, as those elicited by the inactivated virus (Liu *et al.*, 2010). When studies included the C protein (also for DENV) they were able to find correct particle formation (Fu *et al.*, 1997) though the study did not state weather or not the VLPs elicited immunity in a host that was comparable to an inactivated virus. In addition, trials in which VLPs were produced from the prME of JEV showed immunogenicity and protection in mice that were given lethal challenge of JEV (Konishi *et al.*, 1992). These results indicate that inclusion of the C protein in flavivirus VLPs is not necessary to generate a proper host immune response.

In the current study we present the ability to quickly produce ZIKV VLPs that contain the native ZIKV pr, M, and E proteins in *N. benthamia* plants. In addition, we show that these proteins are like the authentic Zika virus in both conformation and approximate size. VLPs in the past have been regarded as promising vaccine candidates due to their ability to self-assemble structures that resemble native viruses. As a result, VLPs are able to present authentic epitopes to the immune system and elicit high titer antibody responses by B-cells through creation of memory B cells or long-lived plasma cells (Chackerian, 2007; Murphy and Weaver, 2016; Zabel *et al.*, 2013).

In recent years, Zika Virus has infected millions of people, has been demonstrated to be a teratogen (including being the causal agent of neurodevelopmental pathologies such as microcephaly afflicting of thousands of babies), and has been

correlated with GBS in adults (Adibi *et al.*, 2016; Cao-Lormeau *et al.*, 2016; Faria *et al.*, 2016; Petersen *et al.*, 2016; Ritter *et al.*, 2017). While the epidemics in South and Central America subsided globally there remain areas with compatible insect vectors and human populations that are naïve to the Brazilian strain of ZIKV (most of Asia, large parts of Africa, southern Europe and the southern US) where ZIKV outbreaks may take pandemic proportions. Moreover, climate change may expand the spread of the mosquito vectors to more northerly areas in the US, Canada and Europe. It is therefore very likely that we have not yet heard the last of ZIKV. The world has been given an amnesty to better prepare for the next wave of ZIKV outbreaks by developing efficacious, cost-effective, safe and globally available prophylactic and therapeutic interventions. The results of this study provide the initial steps to a means that would allow for cost-effective prophylactic intervention of ZIKV.

## 5. FUTURE WORK

If signal is detected in the pellet after incubation with the polyclonal antibodies used in this study then it would be beneficial to add a denaturing reagent to the pellet, such as urea or guanidine in an effort to unfold the protein from its native conformation and to bring the protein into solution (Pace, 1986). After this is complete, the protein could be refolded, as to reform the protein structure. This protein could then be ran through a sucrose gradient to determine if there is presence of the proteins of interest in this study, how dense they are and what size they might be. Such an experiment would allow for optimum protein yield to be achieved.

Determination of the immune response initiated by these VLPs in mice would also be helpful in determining the immunogenicity of the plant produced VLP. Immune cell response assays could be completed as a result of this experiment to determine what the vaccine might do inside of a human host. These immunological assays could include

cytokine assays performed on splenocyte samples post immunization with the VLP. The most cytokines to measure would likely be IFN-gamma, IL-4 and IL-6, as these cytokines are the most likely to be excreted in response to the actual ZIKV (Ball, 1994; Hamel *et al.*, 2015).

The described study sheds light on methods that can be used to develop and isolate Zika VLPs. These developments pave the way for further research in the realm of plant-produced pharmaceuticals and development of therapeutics that can be available to people living in areas with little income and limited access to healthcare.

REFERENCES


Abbink, P., Stephenson, K.E., and Barouch, D.H. (2018) *Zika virus vaccines. Nat. Rev. Microbiol.*, 1.

Acosta-Reyes, J., Navarro, E., Herrera, M.J., Goenaga, E., Ospina, M.L., Parra, E., et al. (2017) *Severe Neurologic Disorders in 2 Fetuses with Zika Virus Infection, Colombia. Emerg. Infect. Dis.*, **23**, 982–984.

Adibi, J.J., Marques, E.T.A., Cartus, A., and Beigi, R.H. (2016) *Teratogenic effects of the Zika virus and the role of the placenta. Lancet*, **387**, 1587–1590.

Aliota, M.T., Caine, E.A., Walker, E.C., Larkin, K.E., Camacho, E., and Osorio, J.E. (2016) *Characterization of Lethal Zika Virus Infection in AG129 Mice. PLoS Negl. Trop. Dis.*, **10**, e0004682.

Araujo, A.Q.C., Silva, M.T.T., and Araujo, A.P.Q.C. (2016) *Zika virus-associated neurological disorders: a review. Brain*, **139**, 2122–2130.

Bachmann, M.F. and Zinkernagel, R.M. (1997) *NEUTRALIZING ANTIVIRAL B CELL RESPONSES. Annu. Rev. Immunol.*, **15**, 235–270.

Ball, L.A. (1994) *Replication of the genomic RNA of a positive-strand RNA animal virus from negative-sense transcripts. Proc. Natl. Acad. Sci. U. S. A.*, **91**, 12443–7.

Baronti, C., Piorkowski, G., Charrel, R.N., Boubis, L., Leparc-Goffart, I., and de Lamballerie, X. (2014) *Complete coding sequence of zika virus from a French polynesia outbreak in 2013. Genome Announc.*, **2**, e00500-14.

Barouch, D.H., Liu, J., Peter, L., Abbink, P., Iampietro, M.J., Cheung, A., et al. (2013) *Characterization of Humoral and Cellular Immune Responses Elicited by a Recombinant Adenovirus Serotype 26 HIV-1 Env Vaccine in Healthy Adults (IPCAVD 001). J. Infect. Dis.*, **207**, 248–256.

Bearcroft, W.G.C. (1956) *Zika virus infection experimentally induced in a human volunteer. Trans. R. Soc. Trop. Med. Hyg.*, **50**, 442–448.

Beasley, D.W.C., Whiteman, M.C., Zhang, S., Huang, C.Y.-H., Schneider, B.S., Smith, D.R., et al. (2005) *Envelope protein glycosylation status influences mouse neuroinvasion phenotype of genetic lineage 1 West Nile virus strains. J. Virol.*, **79**, 8339–47.

Becker, D., Kemper, E., Schell, J., and Masterson, R. (1992) *New plant binary vectors with selectable markers located proximal to the left T-DNA border. Plant Mol. Biol.*, **20**, 1195–1197.

Benelli, G. and Mehlhorn, H. (2016) *Declining malaria, rising of dengue and Zika virus: insights for mosquito vector control. Parasitol. Res.*, **115**, 1747–1754.

Benfey, P.N. and Chua, N.H. (1990) *The Cauliflower Mosaic Virus 35S Promoter: Combinatorial Regulation of Transcription in Plants*. *Science*, **250**, 959–66.

Bertolotti-Ciarlet, A., Ciarlet, M., Crawford, S.E., Conner, M.E., and Estes, M.K. (2003) *Immunogenicity and protective efficacy of rotavirus 2/6-virus-like particles produced by a dual baculovirus expression vector and administered intramuscularly, intranasally, or orally to mice*. *Vaccine*, **21**, 3885–3900.

Besnard, M., Lastère, S., Teissier, A., Cao-Lormeau, V., and Musso, D. (2014) *Evidence of perinatal transmission of Zika virus, French Polynesia, December 2013 and February 2014*. *Eurosurveillance*, **19**, 20751.

Bray, M. and LAl, C. (1991) *Dengue Virus Premembrane and Membrane Proteins Elicit a Protective Immune Response*. **185**, 505–508.

Bright, R.A., Carter, D.M., Daniluk, S., Toapanta, F.R., Ahmad, A., Gavrilov, V., et al. (2007) *Influenza virus-like particles elicit broader immune responses than whole virion inactivated influenza virus or recombinant hemagglutinin*. *Vaccine*, **25**, 3871–3878.

Brito, L.A., Kommareddy, S., Maione, D., Uematsu, Y., Giovani, C., Berlanda Scorza, F., et al. (2015) *Self-Amplifying mRNA Vaccines*. *Adv. Genet.*, **89**, 179–233.

Cao-Lormeau, V.-M., Blake, A., Mons, S., Lastère, S., Roche, C., Vanhomwegen, J., et al. (2016) *Guillain-Barré Syndrome outbreak associated with Zika virus infection in French Polynesia: a case-control study*. *Lancet*, **387**, 1531–1539.

Carter, R.H. and Fearon, D.T. (1992) *CD19: lowering the threshold for antigen receptor stimulation of B lymphocytes*. *Science*, **256**, 105–7.

Center For Disease Control (2018) *Pregnancy Outcomes | Zika and Pregnancy | CDC*.

Chackerian, B. (2007) *Virus-like particles: flexible platforms for vaccine development*. *Expert Rev. Vaccines*, **6**, 381–390.

Chen, Q. and Davis, K.R. (2016) *The potential of plants as a system for the development and production of human biologics*. *F1000Research*, **5**.

Chen, Q., Dent, M., Hurtado, J., Stahnke, J., McNulty, A., Leuzinger, K., and Lai, H. (2016) *Transient Protein Expression by Agroinfiltration in Lettuce*. In: , pp. 55–67. Humana Press, New York, NY.

Christensen, N.D., Dillner, J., Eklund, C., Carter, J.J., Wipf, G.C., Reed, C.A., et al. (1996) *Surface Conformational and Linear Epitopes on HPV-16 and HPV-18 L1 Virus-like Particles as Defined by Monoclonal Antibodies*. *Virology*, **223**, 174–184.

Cinamon, G., Zachariah, M.A., Lam, O.M., Foss, F.W., and Cyster, J.G. (2008) *Follicular shuttling of marginal zone B cells facilitates antigen transport*. *Nat. Immunol.*, **9**, 54–62.

Combredet, C., Labrousse, V., Mollet, L., Lorin, C., Delebecque, F., Hurtrel, B., et al. (2003) *A molecularly cloned Schwarz strain of measles virus vaccine induces strong immune responses in macaques and transgenic mice*. *J. Virol.*, **77**, 11546–54.

Cugola, F.R., Fernandes, I.R., Russo, F.B., Freitas, B.C., Dias, J.L.M., Guimarães, K.P., et al. (2016) *The Brazilian Zika virus strain causes birth defects in experimental models*. *Nature*, **534**, 267–271.

Dai, L., Song, J., Lu, X., Deng, Y.-Q., Musyoki, A.M., Cheng, H., et al. (2016) *Structures of the Zika Virus Envelope Protein and Its Complex with a Flavivirus Broadly Protective Antibody*. *Cell Host Microbe*, **19**, 696–704.

Daniell, H., Singh, N.D., Mason, H., and Streatfield, S.J. (2009) *Plant-made vaccine antigens and biopharmaceuticals*. *Trends Plant Sci.*, **14**, 669–679.

Davidson, A.D. (2009) *Chapter 2 New Insights into Flavivirus Nonstructural Protein 5*. *Adv. Virus Res.*, **74**, 41–101.

Diamos, A.G. and Mason, H.S. (2018a) *Chimeric 3' flanking regions strongly enhance gene expression in plants*. *Plant Biotechnol. J.*

Diamos, A.G. and Mason, H.S. (2018b) *High-level expression and enrichment of norovirus virus-like particles in plants using modified geminiviral vectors*. *Protein Expr. Purif.*, **151**, 86–92.

Dick, G.W.. (1952) *Zika virus (II). Pathogenicity and physical properties*. *Trans. R. Soc. Trop. Med. Hyg.*, **46**, 521–534.

Dick, G.W.., Kitchen, S.., and Haddow, A.. (1952) *Zika Virus (I). Isolations and serological specificity*. *Trans. R. Soc. Trop. Med. Hyg.*, **46**, 509–520.

Duffy, M.R., Chen, T.-H., Hancock, W.T., Powers, A.M., Kool, J.L., Lanciotti, R.S., et al. (2009) *Zika Virus Outbreak on Yap Island, Federated States of Micronesia*. *N. Engl. J. Med.*, **360**, 2536–2543.

Dupont-Rouzeyrol, M., O'Connor, O., Calvez, E., Daurès, M., John, M., Grangeon, J.-P., and Gourinat, A.-C. (2015) *Co-infection with Zika and dengue viruses in 2 patients, New Caledonia, 2014*. *Emerg. Infect. Dis.*, **21**, 381–2.

Elena, S.F. and Sanjuán, R. (2005) *Adaptive value of high mutation rates of RNA viruses: separating causes from consequences*. *J. Virol.*, **79**, 11555–8.

Evens, R. and Kaitin, K. (2015) *The Evolution Of Biotechnology And Its Impact On Health Care*. *Health Aff.*, **34**, 210–219.

Faria, N.R., Azevedo, R. do S. da S., Kraemer, M.U.G., Souza, R., Cunha, M.S., Hill, S.C., et al. (2016) *Zika virus in the Americas: Early epidemiological and genetic*

*findings*. *Science*, **352**, 345–349.

Fibriansah, G., Ng, T.-S., Kostyuchenko, V.A., Lee, J., Lee, S., Wang, J., and Lok, S.-M. (2013) *Structural changes in dengue virus when exposed to a temperature of 37°C*. *J. Virol.*, **87**, 7585–92.

Fischer, R., Stoger, E., Schillberg, S., Christou, P., and Twyman, R.M. (2004) *Plant-based production of biopharmaceuticals*. *Curr. Opin. Plant Biol.*, **7**, 152–158.

Fu, J., Chan, Y.C., Sugrue, R.J., and Howe, J. (1997) *Expression of the dengue virus structural proteins in Pichia pastoris leads to the generation of virus-like particles*. *J. Gen. Virol.*, **78**, 1861–1866.

Garcia, R., Marchette, N.J., and Rudnick, A. (1969) *Isolation of Zika Virus from Aedes Aegypti Mosquitoes in Malaysia *. Am. J. Trop. Med. Hyg.*, **18**, 411–415.

Gheysen, D., Jacobs, E., de Foresta, F., Thiriart, C., Francotte, M., Thines, D., and De Wilde, M. (1989) *Assembly and release of HIV-1 precursor Pr55gag virus-like particles from recombinant baculovirus-infected insect cells*. *Cell*, **59**, 103–112.

Gladwyn-Ng, I., Cordón-Barris, L., Alfano, C., Creppe, C., Couderc, T., Morelli, G., et al. (2018) *Stress-induced unfolded protein response contributes to Zika virus–associated microcephaly*. *Nat. Neurosci.*, **21**, 63–71.

Goncé, A., Martínez, M.J., Marbán-Castro, E., Saco, A., Soler, A., Alvarez-Mora, M.I., et al. (2018) *Spontaneous Abortion Associated with Zika Virus Infection and Persistent Viremia*. *Emerg. Infect. Dis.*, **24**, 933–935.

Gonzalez, S.F., Degn, S.E., Pitcher, L.A., Woodruff, M., Heesters, B.A., and Carroll, M.C. (2011) *Trafficking of B Cell Antigen in Lymph Nodes*. *Annu. Rev. Immunol.*, **29**, 215–233.

GOTO, Y., NIWA, Y., SUZUKI, T., DOHMAE, N., UMEZAWA, K., and SIMIZU, S. (2014) *C-mannosylation of human hyaluronidase 1: Possible roles for secretion and enzymatic activity*. *Int. J. Oncol.*, **45**, 344–350.

Grard, G., Caron, M., Mombo, I.M., Nkoghe, D., Mboui Ondo, S., Jiolle, D., et al. (2014) *Zika Virus in Gabon (Central Africa) – 2007: A New Threat from Aedes albopictus? PLoS Negl. Trop. Dis.*, **8**, e2681.

Grgacic, E.V.L. and Anderson, D.A. (2006) *Virus-like particles: Passport to immune recognition*. *Methods*, **40**, 60–65.

Gubler, D.J. (2002) *The global emergence/resurgence of arboviral diseases as public health problems*. *Arch. Med. Res.*, **33**, 330–42.

Gupta, A.K., Kaur, K., Rajput, A., Dhanda, S.K., Sehgal, M., Khan, M.S., et al. (2016) *ZikaVR: An Integrated Zika Virus Resource for Genomics, Proteomics, Phylogenetic and Therapeutic Analysis*. *Sci. Rep.*, **6**, 32713.

Hadden, R.D.M. and Gregson, N.A. (2001) *Guillain-Barre syndrome and Campylobacter jejuni infection*. *J. Appl. Microbiol.*, **90**, 145S–154S.

Halstead, S.B. (2003) *The Flaviviruses: Pathogenesis and Immunity - Google Books*. *Adv. Virus Res.*, 421–423.

Hamel, R., Dejarnac, O., Wichit, S., Ekchariyawat, P., Neyret, A., Luplertlop, N., et al. (2015) *Biology of Zika Virus Infection in Human Skin Cells*. *J. Virol.*, **89**, 8880–96.

Hanly, W.C., Artwohl, J.E., and Bennett, B.T. (1995) *Review of Polyclonal Antibody Production Procedures in Mammals and Poultry*. *ILAR J.*, **37**, 93–118.

Harrison, S.C. (2008) *Viral membrane fusion*. *Nat. Struct. Mol. Biol.*, **15**, 690–698.

Hasan, S.S., Sevvana, M., Kuhn, R.J., and Rossmann, M.G. (2018) *Structural biology of Zika virus and other flaviviruses*. *Nat. Struct. Mol. Biol.*, **25**, 13–20.

Heinz, F.X., Stiasny, K., Püschner-Auer, G., Holzmann, H., Allison, S.L., Mandl, C.W., and Kunz, C. (1994) *Structural Changes and Functional Control of the Tick-Borne Encephalitis Virus Glycoprotein E by the Heterodimeric Association with Protein prM*. *Virology*, **198**, 109–117.

Hennessey, M., Fischer, M., and Staples, J.E. (2016) *Zika Virus Spreads to New Areas - Region of the Americas, May 2015-January 2016*. *Am. J. Transplant.*, **16**, 1031–1034.

Hsieh, Y.-C., Omarov, R.T., and Scholthof, H.B. (2009) *Diverse and newly recognized effects associated with short interfering RNA binding site modifications on the Tomato bushy stunt virus p19 silencing suppressor*. *J. Virol.*, **83**, 2188–200.

Huang, Z., Chen, Q., Hjelm, B., Arntzen, C., and Mason, H. (2009) *A DNA replicon system for rapid high-level production of virus-like particles in plants*. *Biotechnol. Bioeng.*, **103**, 706–714.

Kang, D., Gopalkrishnan, R. V, Wu, Q., Jankowsky, E., Pyle, A.M., Fisher, P.B., and Randall, R.E. (2002) *mda-5: An interferon-inducible putative RNA helicase with double-stranded RNA-dependent ATPase activity and melanoma growth-suppressive properties*. *Proc. Natl. Acad. Sci. U. S. A.*, **99**, 637–42.

Kapila, J., De Rycke, R., Van Montagu, M., and Angenon, G. (1997) *An Agrobacterium-mediated transient gene expression system for intact leaves*. *Plant Sci.*, **122**, 101–108.

Kaufmann, B., Chipman, P.R., Holdaway, H.A., Johnson, S., Fremont, D.H., Kuhn, R.J., et al. (2009) *Capturing a Flavivirus Pre-Fusion Intermediate*. *PLoS Pathog.*, **5**, e1000672.

Kawai, T., Takahashi, K., Sato, S., Coban, C., Kumar, H., Kato, H., et al. (2005) *IPS-1, an*

*adaptor triggering RIG-I- and Mda5-mediated type I interferon induction. Nat. Immunol.*, **6**, 981–988.

Konishi, E., Fujii, A., and Mason, P.W. (2001) *Generation and characterization of a mammalian cell line continuously expressing Japanese encephalitis virus subviral particles. J. Virol.*, **75**, 2204–12.

Konishi, E., Pincus, S., Paoletti, E., Shope, R.E., Burrage, T., and Mason, P.W. (1992) *Mice immunized with a subviral particle containing the Japanese encephalitis virus prM/M and E proteins are protected from lethal JEV infection. Virology*, **188**, 714–20.

Konishi, E., Yamaoka, M., Kurane, I., and Mason, P.W. (1998) *Induction of Protective Immunity against Japanese Encephalitis in Mice by Immunization with a Plasmid Encoding Japanese Encephalitis Virus Premembrane and Envelope Genes. J. Virol.*, **72**, 4925–4930.

Kostyuchenko, V.A., Lim, E.X.Y., Zhang, S., Fibriansah, G., Ng, T.-S., Ooi, J.S.G., et al. (2016) *Structure of the thermally stable Zika virus. Nature*, **533**, 425–428.

Krenek, P., Samajova, O., Luptovciak, I., Doskocilova, A., Komis, G., and Samaj, J. (2015) *Transient plant transformation mediated by Agrobacterium tumefaciens: Principles, methods and applications. Biotechnol. Adv.*, **33**, 1024–1042.

Krow-Lucal, E.R., Biggerstaff, B.J., and Staples, J.E. (2017) *Estimated Incubation Period for Zika Virus Disease. Emerg. Infect. Dis.*, **23**, 841–845.

Kuhn, R.J., Zhang, W., Rossmann, M.G., Pletnev, S. V., Corver, J., Lenches, E., et al. (2002) *Structure of Dengue Virus: Implications for Flavivirus Organization, Maturation, and Fusion. Cell*, **108**, 717–725.

Lacroix, B. and Citovsky, V. (2013) *The roles of bacterial and host plant factors in Agrobacterium-mediated genetic transformation. Int. J. Dev. Biol.*, **57**, 467–81.

Laguesse, S., Creppe, C., Nedialkova, D.D., Prévot, P.-P., Borgs, L., Huysseune, S., et al. (2015) *A Dynamic Unfolded Protein Response Contributes to the Control of Cortical Neurogenesis. Dev. Cell*, **35**, 553–567.

Lauer, K.B., Borrow, R., and Blanchard, T.J. (2017) *Multivalent and Multipathogen Viral Vector Vaccines. Clin. Vaccine Immunol.*, **24**, e00298-16.

Lee, L.-Y. and Gelvin, S.B. (2008) *T-DNA binary vectors and systems. Plant Physiol.*, **146**, 325–32.

Leung, G.H., Baird, R.W., Druce, J., Anstey, N.M., and Darwin Hospital, R. (2015) *Zika Virus infection in Australia Following a Monkey Bite in Indonesia. J trop Med public Heal.*, **460**.

Li, H., Saucedo-Cuevas, L., Regla-Nava, J.A., Chai, G., Sheets, N., Tang, W., et al. (2016)

*Zika Virus Infects Neural Progenitors in the Adult Mouse Brain and Alters Proliferation*. *Cell Stem Cell*, **19**, 593–598.

Li, L., Lok, S.-M., Yu, I.-M., Zhang, Y., Kuhn, R.J., Chen, J., and Rossmann, M.G. (2008) *The flavivirus precursor membrane-envelope protein complex: structure and maturation*. *Science*, **319**, 1830–4.

Liu, W., Jiang, H., Zhou, J., Yang, X., Tang, Y., Fang, D., and Jiang, L. (2010) *Recombinant dengue virus-like particles from Pichia pastoris: efficient production and immunological properties*. *Virus Genes*, **40**, 53–59.

Lorenz, I.C., Allison, S.L., Heinz, F.X., and Helenius, A. (2002) *Folding and dimerization of tick-borne encephalitis virus envelope proteins prM and E in the endoplasmic reticulum*. *J. Virol.*, **76**, 5480–91.

Madera, S., Rapp, M., Firth, M.A., Beilke, J.N., Lanier, L.L., and Sun, J.C. (2016) *Type I IFN promotes NK cell expansion during viral infection by protecting NK cells against fratricide*. *J. Exp. Med.*, **213**, 225–33.

Magira, E.E., Papaioakim, M., Nachamkin, I., Asbury, A.K., Li, C.Y., Ho, T.W., et al. (2003) *Differential distribution of HLA-DQ beta/DR beta epitopes in the two forms of Guillain-Barré syndrome, acute motor axonal neuropathy and acute inflammatory demyelinating polyneuropathy (AIDP): identification of DQ beta epitopes associated with susceptibility to and protection from AIDP*. *J. Immunol.*, **170**, 3074–80.

Mansuy, J.M., Dutertre, M., Mengelle, C., Fourcade, C., Marchou, B., Delobel, P., et al. (2016) *Zika virus: high infectious viral load in semen, a new sexually transmitted pathogen?*

Marques, E.T.A. and Burke, D.S. (2018) *Tradition and innovation in development of a Zika vaccine*. *Lancet (London, England)*, **391**, 516–517.

Matsuo, K., Fukuzawa, N., and Matsumura, T. (2016) *A simple agroinfiltration method for transient gene expression in plant leaf discs*. *J. Biosci. Bioeng.*, **122**, 351–356.

McCormick, A.A., Reddy, S., Reinl, S.J., Cameron, T.I., Czerwinkski, D.K., Vojdani, F., et al. (2008) *Plant-produced idiotype vaccines for the treatment of non-Hodgkin's lymphoma: Safety and immunogenicity in a phase I clinical study*. *Proc. Natl. Acad. Sci.*, **105**, 10131–10136.

Meertens, L., Labeau, A., Dejarnac, O., Cipriani, S., Sinigaglia, L., Bonnet-Madin, L., et al. (2017) *Axl Mediates ZIKA Virus Entry in Human Glial Cells and Modulates Innate Immune Responses*. *Cell Rep.*, **18**, 324–333.

Milligan, I.D., Gibani, M.M., Sewell, R., Clutterbuck, E.A., Campbell, D., Plested, E., et al. (2016) *Safety and Immunogenicity of Novel Adenovirus Type 26– and Modified Vaccinia Ankara–Vectored Ebola Vaccines*. *JAMA*, **315**, 1610.

MILSTEIN, C., BROWNLEE, G.G., HARRISON, T.M., and MATHEWS, M.B. (1972) *A Possible Precursor of Immunoglobulin Light Chains*. *Nat. New Biol.*, **239**, 117–120.

Mlakar, J., Korva, M., Tul, N., Popović, M., Poljšak-Prijatelj, M., Mraz, J., et al. (2016) *Zika Virus Associated with Microcephaly*. *N. Engl. J. Med.*, **374**, 951–958.

Modjarrad, K., Lin, L., George, S.L., Stephenson, K.E., Eckels, K.H., De La Barrera, R.A., et al. (2018) *Preliminary aggregate safety and immunogenicity results from three trials of a purified inactivated Zika virus vaccine candidate: phase 1, randomised, double-blind, placebo-controlled clinical trials*. *Lancet (London, England)*, **391**, 563–571.

Monath, T.P. (2018) *Chikungunya and Zika: The Future*. In: *Chikungunya and Zika Viruses* , pp. 367–377. Elsevier.

Mor, T.S., Moon, Y.-S., Palmer, K.E., and Mason, H.S. (2003) *Geminivirus vectors for high-level expression of foreign proteins in plant cells*. *Biotechnol. Bioeng.*, **81**, 430–437.

Mukhopadhyay, S., Kuhn, R.J., and Rossmann, M.G. (2005) *A structural perspective of the flavivirus life cycle*. *Nat. Rev. Microbiol.*, **3**, 13–22.

Murphy, K. and Weaver, C. (2016) *Janeway's Immunobiology*. Garland Science.

Murray, C.L., Jones, C.T., and Rice, C.M. (2008) *Architects of assembly: roles of Flaviviridae non-structural proteins in virion morphogenesis*. *Nat. Rev. Microbiol.*, **6**, 699–708.

Musso, D., Nhan, T., Robin, E., Roche, C., Bierlaire, D., Zisou, K., et al. (2014) *Potential for Zika virus transmission through blood transfusion demonstrated during an outbreak in French Polynesia, November 2013 to February 2014*. *Eurosurveillance*, **19**, 20761.

Nguyen, S.M., Antony, K.M., Dudley, D.M., Kohn, S., Simmons, H.A., Wolfe, B., et al. (2017) *Highly efficient maternal-fetal Zika virus transmission in pregnant rhesus macaques*. *PLOS Pathog.*, **13**, e1006378.

Noad, R. and Roy, P. (2003) *Virus-like particles as immunogens*. *Trends Microbiol.*, **11**, 438–444.

Noll, H. and Noll, M. (1989) *[5] Sucrose gradient techniques and applications to nucleosome structure*. *Methods Enzymol.*, **170**, 55–116.

Oehler, E., Watrin, L., Larre, P., Leparc-Goffart, I., Lastère, S., Valour, F., et al. (2014) *Zika virus infection complicated by Guillain-Barré syndrome – case report, French Polynesia, December 2013*. *Eurosurveillance*, **19**, 20720.

Olson, J.G., Ksiazek, T.G., Suhandiman, and Triwibowo (1981) *Zika virus, a cause of fever in Central Java, Indonesia*. *Trans. R. Soc. Trop. Med. Hyg.*, **75**, 389–393.

Pace, C. (1986) *Determination and Analysis of Urea and Guanidine Hydrochloride Denaturation Curves*. *Methods Enzymol.*, 267–270.

Pardi, N., Hogan, M.J., Pelc, R.S., Muramatsu, H., Andersen, H., DeMaso, C.R., et al. (2017) *Zika virus protection by a single low-dose nucleoside-modified mRNA vaccination*. *Nature*, **543**, 248–251.

Paul, L.M., Carlin, E.R., Jenkins, M.M., Tan, A.L., Barcellona, C.M., Nicholson, C.O., et al. (2016) *Dengue virus antibodies enhance Zika virus infection*. *Clin. Transl. Immunol.*, **5**, e117.

Paz-Bailey, G., Rosenberg, E.S., Doyle, K., Munoz-Jordan, J., Santiago, G.A., Klein, L., et al. (2017) *Persistence of Zika Virus in Body Fluids — Preliminary Report*. *N. Engl. J. Med.*, NEJMoa1613108.

Petersen, L.R., Jamieson, D.J., Powers, A.M., and Honein, M.A. (2016) *Zika Virus*. *N. Engl. J. Med.*, **374**, 1552–1563.

Phi-Van, L., von Kries, J.P., Ostertag, W., and Strätling, W.H. (1990) *The chicken lysozyme 5' matrix attachment region increases transcription from a heterologous promoter in heterologous cells and dampens position effects on the expression of transfected genes*. *Mol. Cell. Biol.*, **10**, 2302–7.

Pichlmair, A., Schulz, O., Tan, C.-P., Rehwinkel, J., Kato, H., Takeuchi, O., et al. (2009) *Activation of MDA5 Requires Higher-Order RNA Structures Generated during Virus Infection*. *J. Virol.*, **83**, 10761–10769.

Plevka, P., Battisti, A.J., Junjhon, J., Winkler, D.C., Holdaway, H.A., Keelapang, P., et al. (2011) *Maturation of flaviviruses starts from one or more icosahedrally independent nucleation centres*. *EMBO Rep.*, **12**, 602–606.

Ponlawat, A. and Harrington, L.C. (2009) *Blood Feeding Patterns of Aedes aegypti and Aedes albopictus in Thailand*. *http://dx.doi.org/10.1603/0022-2585(2005)042[0844:BFPOAA]2.0.CO;2*.

Ponting, C.P., Hutton, M., Nyborg, A., Baker, M., Jansen, K., and Golde, T.E. (2002) *Identification of a novel family of presenilin homologues*. *Hum. Mol. Genet.*, **11**, 1037–1044.

Priyamvada, L., Suthar, M.S., Ahmed, R., and Wrammert, J. (2017) *Humoral Immune Responses Against Zika Virus Infection and the Importance of Preexisting Flavivirus Immunity*. *J. Infect. Dis.*, **216**, S906–S911.

Rasmussen, S.A., Jamieson, D.J., Honein, M.A., and Petersen, L.R. (2016) *Zika Virus and Birth Defects — Reviewing the Evidence for Causality*. *N. Engl. J. Med.*, **374**, 1981–1987.

Rastogi, M., Sharma, N., and Singh, S.K. (2016) *Flavivirus NS1: a multifaceted*

*enigmatic viral protein. Virol. J.*, **13**, 131.

Reichmuth, A.M., Oberli, M.A., Jaklenec, A., Langer, R., and Blankschtein, D. (2016) *mRNA vaccine delivery using lipid nanoparticles. Ther. Deliv.*, **7**, 319–334.

Richard, A.S., Shim, B.-S., Kwon, Y.-C., Zhang, R., Otsuka, Y., Schmitt, K., et al. (2017) *AXL-dependent infection of human fetal endothelial cells distinguishes Zika virus from other pathogenic flaviviruses. Proc. Natl. Acad. Sci. U. S. A.*, **114**, 2024–2029.

Richner, J.M., Himansu, S., Dowd, K.A., Butler, S.L., Salazar, V., Fox, J.M., et al. (2017) *Modified mRNA Vaccines Protect against Zika Virus Infection. Cell*, **168**, 1114–1125.e10.

Ritter, J.M., Martines, R.B., and Zaki, S.R. (2017) *Zika Virus: Pathology From the Pandemic. Arch. Pathol. Lab. Med.*, **141**, 49–59.

Rivera, A.L., Gómez-Lim, M., Fernández, F., and Loske, A.M. (2012) *Physical methods for genetic plant transformation. Phys. Life Rev.*, **9**, 308–345.

Roth, A., Mercier, A., Lepers, C., Hoy, D., Duituturaga, S., Benyon, E., et al. (2014) *Concurrent outbreaks of dengue, chikungunya and Zika virus infections – an unprecedented epidemic wave of mosquito-borne viruses in the Pacific 2012–2014. Eurosurveillance*, **19**, 20929.

Salvo, M.A., Kingstad-Bakke, B., Salas-Quinchucua, C., Camacho, E., and Osorio, J.E. (2018) *Zika virus like particles elicit protective antibodies in mice. PLoS Negl. Trop. Dis.*, **12**, e0006210.

Santi, L., Huang, Z., and Mason, H. (2006) *Virus-like particles production in green plants. Methods*, **40**, 66–76.

Schaller, A. and Ryan, C.A. (1996) *Systemin - a polypeptide defense signal in plants. BioEssays*, **18**, 27–33.

Schuler-Faccini, L., Ribeiro, E.M., Feitosa, I.M.L., Horovitz, D.D.G., Cavalcanti, D.P., Pessoa, A., et al. (2016) *Possible Association Between Zika Virus Infection and Microcephaly — Brazil, 2015. MMWR. Morb. Mortal. Wkly. Rep.*, **65**, 59–62.

Simpson, D.I.H. (1964) *Zika virus infection in man. Trans. R. Soc. Trop. Med. Hyg.*, **58**, 335–338.

Sirohi, D., Chen, Z., Sun, L., Klose, T., Pierson, T.C., Rossmann, M.G., and Kuhn, R.J. (2016) *The 3.8 Å resolution cryo-EM structure of Zika virus. Science*, **352**, 467–70.

Sotelo, J.R., Sotelo, A.B., Sotelo, F.J.B., Doi, A.M., Pinho, J.R.R., Oliveira, R. de C., et al. (2017) *Persistence of Zika Virus in Breast Milk after Infection in Late Stage of Pregnancy. Emerg. Infect. Dis.*, **23**, 856–857.

Steen, P. Van den, Rudd, P.M., Dwek, R.A., and Opdenakker, G. (1998) *Concepts and Principles of O-Linked Glycosylation*. *Crit. Rev. Biochem. Mol. Biol.*, **33**, 151–208.

Takada, A. and Kawaoka, Y. (2003) *Antibody-dependent enhancement of viral infection: molecular mechanisms andin vivo implications*. *Rev. Med. Virol.*, **13**, 387–398.

Tebas, P., Roberts, C.C., Muthumani, K., Reuschel, E.L., Kudchodkar, S.B., Zaidi, F.I., et al. (2017) *Safety and Immunogenicity of an Anti–Zika Virus DNA Vaccine — Preliminary Report*. *N. Engl. J. Med.*, NEJMoa1708120.

Tognarelli, J., Ulloa, S., Villagra, E., Lagos, J., Aguayo, C., Fasce, R., et al. (2016) *A report on the outbreak of Zika virus on Easter Island, South Pacific, 2014*. *Arch. Virol.*, **161**, 665–668.

Uematsu, S. and Akira, S. (2007) *Toll-like receptors and Type I interferons*. *J. Biol. Chem.*, **282**, 15319–23.

Uhlén, M., Fagerberg, L., Hallström, B.M., Lindskog, C., Oksvold, P., Mardinoglu, A., et al. (2015) *Proteomics. Tissue-based map of the human proteome*. *Science*, **347**, 1260419.

United Nations Development Programme (2017) *A Socio-economic Impact Assessment of the Zika Virus in Latin America and the Caribbean | UNDP*. *United Nations Dev. Program.*

Ura, T., Okuda, K., and Shimada, M. (2014) *Developments in Viral Vector-Based Vaccines*. *Vaccines*, **2**, 624–41.

Van Veldhoven, P.P., Baumgart, E., and Mannaerts, G.P. (1996) *Iodixanol (Optiprep), an Improved Density Gradient Medium for the Iso-osmotic Isolation of Rat Liver Peroxisomes*. *Anal. Biochem.*, **237**, 17–23.

Vigerust, D.J. and Shepherd, V.L. (2007) *Virus glycosylation: role in virulence and immune interactions*. *Trends Microbiol.*, **15**, 211–218.

Voss, M., Schröder, B., and Fluhrer, R. (2013) *Mechanism, specificity, and physiology of signal peptide peptidase (SPP) and SPP-like proteases*. *Biochim. Biophys. Acta - Biomembr.*, **1828**, 2828–2839.

Weaver, S.C., Costa, F., Garcia-Blanco, M.A., Ko, A.I., Ribeiro, G.S., Saade, G., et al. (2016) *Zika virus: History, emergence, biology, and prospects for control*. *Antiviral Res.*, **130**, 69–80.

White, J.M., Delos, S.E., Brecher, M., and Schornberg, K. (2008) *Structures and mechanisms of viral membrane fusion proteins: multiple variations on a common theme*. *Crit. Rev. Biochem. Mol. Biol.*, **43**, 189–219.

Yang, M., Sun, H., Lai, H., Hurtado, J., and Chen, Q. (2018) *Plant-produced Zika virus*

*envelope protein elicits neutralizing immune responses that correlate with protective immunity against Zika virus in mice*. *Plant Biotechnol. J.*, **16**, 572–580.

Yu, I.-M., Holdaway, H.A., Chipman, P.R., Kuhn, R.J., Rossmann, M.G., and Chen, J. (2009) *Association of the pr peptides with dengue virus at acidic pH blocks membrane fusion*. *J. Virol.*, **83**, 12101–7.

Yuki, N. (2015) *[Molecular Mimicry and Guillain-Barré Syndrome]*. *Brain Nerve*, **67**, 1341–6.

Zabel, F., Kündig, T.M., and Bachmann, M.F. (2013) *Virus-induced humoral immunity: on how B cell responses are initiated*. *Curr. Opin. Virol.*, **3**, 357–362.

Zanluca, C., Melo, V.C.A. de, Mosimann, A.L.P., Santos, G.I.V. dos, Santos, C.N.D. dos, Luz, K., et al. (2015) *First report of autochthonous transmission of Zika virus in Brazil*. *Mem. Inst. Oswaldo Cruz*, **110**, 569–572.

Zhang, W., Chipman, P.R., Corver, J., Johnson, P.R., Zhang, Y., Mukhopadhyay, S., et al. (2003) *Visualization of membrane protein domains by cryo-electron microscopy of dengue virus*. *Nat. Struct. Mol. Biol.*, **10**, 907–912.

Zhang, Y., Corver, J., Chipman, P.R., Zhang, W., Pletnev, S. V, Sedlak, D., et al. (2003) *Structures of immature flavivirus particles*. *EMBO J.*, **22**, 2604–13.

ZIKAVAX *Home | zikavax*.